

Knotted surfaces in 4-manifolds and their diagrams

Mark Hughes^[0000-0001-6305-2949]

Abstract The study of knotted surfaces in 4-space is a natural generalization of the theory of classical knots and links. In the 4-dimensional setting special techniques are needed for a 3-dimensional mathematician to describe and manipulate these surfaces, similar to how knot theorists use knot projections and Reidemeister moves to study knot diagrams on a 2-dimensional plane. These lectures notes give an introduction to knotted surfaces and some different techniques used to study them, focusing primarily on banded unlink diagrams in S^4 and other closed 4-manifolds.

1 Introduction to knotted surfaces

About these notes

These lecture notes were developed as part of a graduate mini-course taught by the author at the 2024 Georgia Topology Conference at the University of Georgia. The purpose of this mini-course was to introduce students to diagrammatic techniques used to describe knotted surfaces in 4-space, along with isotopies between them. While there are certainly other excellent (and much more complete) references on the theory of knotted surfaces and their diagrams (see, e.g. [4, 5, 10, 11]), these references focus primarily on surfaces in the 4-sphere. The primary goal of these notes will therefore be to develop the theory of banded unlink diagrams, which can be adapted to study knotted surfaces in arbitrary smooth, closed 4-dimensional manifolds and isotopies between them.

We assume no prior knowledge of knotted surfaces, though some familiarity with classical knot theory will be helpful. Some experience with differential topology will also be useful, including concepts such as embeddings, immersions, transversality, Morse functions, and tubular neighborhoods. As our goals include explicitly

Mark Hughes
Brigham Young University, Provo Utah 84602 e-mail: hughes@mathematics.byu.edu

describing surfaces in smooth closed 4-manifolds, the reader will benefit from some background with 4-dimensional handlebody (Kirby) diagrams, though we will review these later.

We proceed as follows: In Section 1 we introduce the idea of a *knotted surface* in S^4 , and give examples by defining several important families of knotted surfaces. We also discuss how knotted surfaces can be described by way of *broken surface diagrams*, which are an immediate analogue of classical knot diagrams in the plane. In Section 2 we discuss *motion picture diagrams* of knotted surfaces, and show how the relevant information in such a diagram can be encoded in a single cross-section of the surface, called a *banded unlink diagram*. We also present *Swenton's Theorem*, which provides a set of moves that are sufficient to relate the banded unlink diagrams of any two isotopic surfaces. Finally, in Section 3, after a brief detour to discuss handle decompositions of 4-manifolds, we generalize the idea of a banded unlink diagram to surfaces in arbitrary smooth closed 4-manifolds. We also reformulate Swenton's theorem in this setting, and show how these ideas can also be used to describe immersed surfaces in 4-manifolds.

As this mini-course was taught through a combination of lectures and interactive problem sessions, many of the concrete examples are posed as homework problems at the end of each section. The interested reader is encouraged to try working through them.

In what follows, we will let $B^n = \{(x_1, \dots, x_n) \in \mathbb{R}^n \mid x_1^2 + \dots + x_n^2 \leq 1\}$ denote the n -dimensional ball, and $S^n = \{(x_1, \dots, x_{n+1}) \in \mathbb{R}^{n+1} \mid x_1^2 + \dots + x_{n+1}^2 = 1\}$ the n -dimensional sphere. If $m < n$, we can think of B^m as sitting inside of B^n by identifying B^m with the set $\{(x_1, \dots, x_n) \in B^n \mid x_{m+1} = x_{m+2} = \dots = x_n = 0\}$, which we refer to as the *standard m -ball* in B^n . We define the *standard m -sphere* in S^n in a similar way, as the set $\{(x_1, \dots, x_{n+1}) \in S^n \mid x_{m+2} = x_{m+3} = \dots = x_{n+1} = 0\}$.

1.1 Knotted and unknotted surfaces

We are ready to jump right in, by immediately defining our main object of interest:

Definition 1 A *knotted surface* (or *surface knot*) is a smooth embedding $K : F^2 \hookrightarrow S^4$, where F^2 is a closed (compact, without boundary) surface. If F^2 is homeomorphic to the 2-sphere S^2 , then K is sometimes called a *2-knot*.

It will often be convenient for us to identify a knotted surface K with its image $K = K(F)$ in S^4 , when there is no risk of this causing confusion. Indeed, for any two smooth embeddings $K, K' : F \hookrightarrow S^4$ with $K(F) = K'(F)$ we can find a diffeomorphism $\sigma : F \rightarrow F$ such that $K \circ \sigma = K'$. Hence we can think of K and K' as differing by a smooth reparametrization.

Example 1 The standard S^2 in S^4 is a knotted surface (admittedly not the most exciting example, but we'll need additional techniques to describe more interesting examples).

Because a knotted surface $K : F \hookrightarrow S^4$ is assumed to be smooth, its image $K = K(F) \subseteq S^4$ is *locally-flat*; in other words every $p \in K$ is contained in an open neighborhood $U \subseteq S^4$ such that the pair $(U, U \cap K)$ is homeomorphic to the standard pair (B^4, B^2) .

To obtain a first non-example of a knotted surface, consider the classical trefoil knot L sitting inside the 3-sphere S^3 . As the suspension of an n -sphere is an $(n + 1)$ -sphere, taking the suspension of the pair (S^3, L) gives a pair $(S(S^3), S(L)) \cong (S^4, S(L))$. Here, $S(L)$ is homeomorphic to S^2 , however it is not embedded locally-flatly in S^4 . Indeed, if U is any 4-ball neighborhood of a cone point of $S(L)$ whose boundary intersects $S(L)$ transversely, then $\partial U \cap S(L)$ will contain a trefoil component $L \subseteq \partial U \cong S^3$. Since L is knotted, the pair $(\partial U, \partial U \cap S(L))$ is not homeomorphic to the standard pair $(S^3, S^1) \cong (\partial B^4, \partial B^2)$, which demonstrates that the cone points of $S(L)$ are not embedded locally-flatly. Thus $S(L)$ is not the image of a smooth knotted surface.

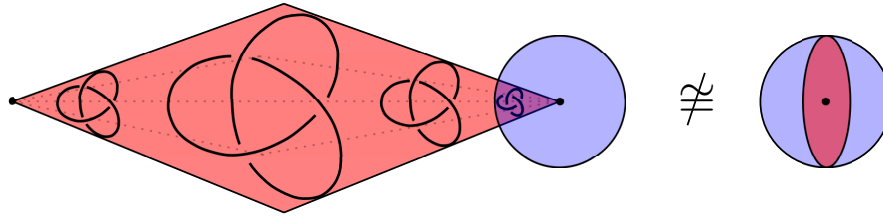


Fig. 1 The cone points of the suspension of a nontrivial classical knot in S^3 are not locally-flat.

Definition 2 Two knotted surfaces $K_1 : F_1 \hookrightarrow S^4$ and $K_2 : F_2 \hookrightarrow S^4$ are *equivalent* if there exists a smooth isotopy $\varphi : [0, 1] \times S^4 \rightarrow S^4$ with $\varphi(1, K_1(F_1)) = K_2(F_2)$.

Thus, two knotted surfaces are equivalent if the image of one of them can continuously be deformed through diffeomorphisms of the ambient space to agree with the other.

As in the classical setting, we need to define what it means for a knotted surface to be “unknotted”. To do this, we turn to the classical setting for inspiration. Specifically, recall that the unknot is the only knot in S^3 which can be isotoped to lie entirely on the standard 2-sphere S^2 (attempting to isotope any other knot to the standard S^2 will necessarily create double points, corresponding to crossings of the resulting knot diagram). This leads to our first definition of unknottedness for orientable knotted surfaces:

Definition 3 An orientable knotted surface in S^4 is *unknotted* if it is equivalent to a knotted surface which lies entirely in the standard $S^3 \subseteq S^4$.

Note that since the standard S^2 in S^4 lies within the standard S^3 , any surface knot which is equivalent to the standard S^2 is unknotted (as reason dictates it should be).

Alternatively, in S^3 the unknot is the only knot that bounds an embedded disk (i.e., the simplest possible surface with boundary). While we could use similar thinking to define an unknotted 2-knot in S^4 to be one which bounds an embedded 3-ball, for higher genus knotted surfaces we need a simple 3-manifold whose boundary has nonzero genus. One simple class of 3-manifolds with boundary are those consisting of only 0 and 1-handles, which we refer to as *3-dimensional 1-handlebodies*. Handles are discussed in the 4-dimensional setting in Section 3.1. For now, you can think of a 3-dimensional 1-handlebody as being obtained by taking a 3-ball B^3 and attaching some number of solid tubes to the boundary in an orientation-preserving manner (see Figure 2, right). The solid torus $S^1 \times D^2$ is a 3-dimensional 1-handlebody, and any 3-dimensional 1-handlebodies can be obtained by taking boundary sums of B^3 with some number of $S^1 \times D^2$.

This leads to our second, equivalent, definition of unknottedness for knotted surfaces:

Definition 4 An orientable knotted surface in S^4 is *unknotted* if it is the boundary of a 3-dimensional 1-handlebody H embedded in S^4 .

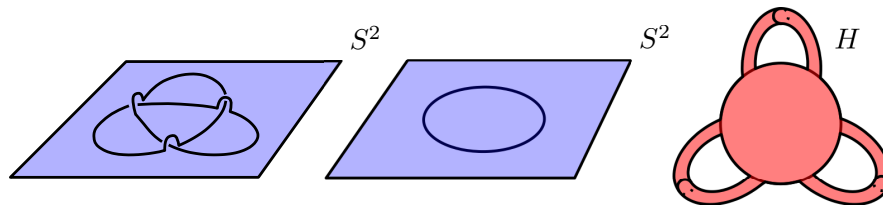


Fig. 2 *Left and center:* The unknot in S^3 is the only knot which can be isotoped to lie in the standard 2-sphere $S^2 \subseteq S^3$, and the only knot in S^3 which bounds a disk. *Right:* A genus 3-handlebody H , whose boundary is an unknotted surface of genus 3.

It can be shown that for orientable surface knots Definitions 3 and 4 are equivalent (see Exercise 1.4). We call any orientable surface which satisfies these equivalent definitions *unknotted*. We will define unknottedness for nonorientable surfaces in Exercise 2.3.

It may be worth noting that unknotted surfaces may sometimes look knotted at first glance. Consider the two knotted surfaces in Figure 3. Here, we have drawn two surfaces in S^3 , which we think of as being the standard S^3 in S^4 . Because both surfaces can be isotoped to lie in S^3 they are both unknotted by Definition 3. Moreover, they both bound embedded 3-dimensional 1-handlebodies and hence are also unknotted by Definition 4. Indeed, although the knotted surfaces in Figure 3 are not isotopic to each other in S^3 they are both unknotted in S^4 , and are equivalent to each other as surfaces in S^4 . Any isotopy relating these two surfaces necessarily must push one of the surfaces at least partially outside of S^3 to make them agree (see Exercise 1.1).

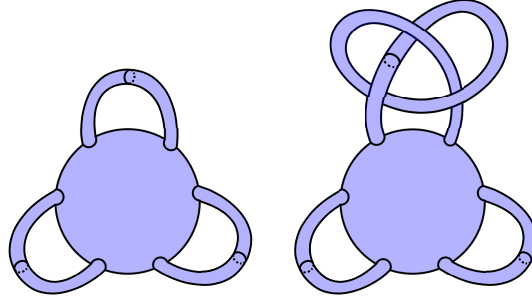


Fig. 3 Two genus 3 knotted surfaces. We've drawn them both in S^3 , which implies that they are both unknotted and equivalent to each other. Isotoping either one of them to the other requires pushing the surface outside of S^3 at some point in the isotopy.

1.2 Broken surface diagrams

Without additional techniques we are somewhat limited in the examples of knotted surfaces we can describe, and what we can do with them. In this section we'll describe our first set of diagrammatic tools for representing and manipulating knotted surfaces. The following techniques are directly analogous to the classical approach of representing a knot in 3-space by first projecting it to the plane, and then breaking one strand at each crossing to record the relative heights of the crossing strands.

We begin by identifying \mathbb{R}^4 with a punctured S^4 , and letting

$$\pi : S^4 \setminus \{\text{pt}\} \cong \mathbb{R}^4 \rightarrow \mathbb{R}^3$$

be a projection of \mathbb{R}^4 onto \mathbb{R}^3 . Let K be a knotted surface in $S^4 \setminus \{\text{pt}\} \cong \mathbb{R}^4$. After a small perturbation, we can arrange K so that its image under π is a generic surface in \mathbb{R}^3 . In other words, after a small perturbation every point p in $\pi(K)$ will have a neighborhood U such that $(U, U \cap \pi(K))$ is diffeomorphic to one of the following local models:

1. $(B^3, \{(x, y, z) \in B^3 \mid z = 0\})$, the xy -plane in B^3 ,
2. $(B^3, \{(x, y, z) \in B^3 \mid yz = 0\})$, the union of the xy - and xz -planes in B^3 ,
3. $(B^3, \{(x, y, z) \in B^3 \mid xyz = 0\})$, the union of the three coordinate planes in B^3 ,
4. $(B^3, \{(x, y, z) \in B^3 \mid x^2 = y^2z\})$, a Whitney umbrella.

Notice that aside from the first model above, each of the remaining local pictures contain arcs of self-intersections of the surface $\pi(K)$. Each arc corresponds to the transverse intersection of two or more sheets of K which coincide under the projection π . (Note that although the central point of the Whitney umbrella is not a double point, it is in the closure of such a double point arc.) Along the double point arcs we can record the relative heights of the two intersecting sheets with respect to π by adding a break along the lower of the two sheets.

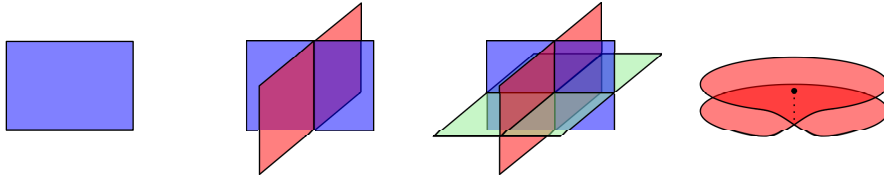


Fig. 4 Local models of the surface $\pi(K)$ in \mathbb{R}^3 . The four models include three that consist of intersections of coordinate planes, and one local model of the Whitney umbrella.

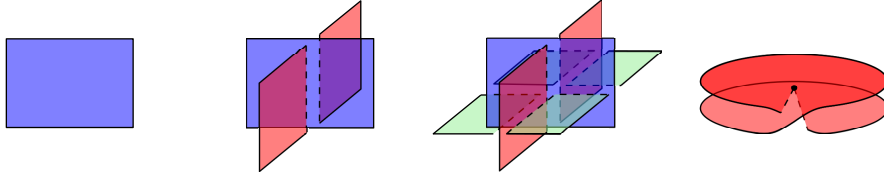


Fig. 5 Local models of the surface $\pi(K)$ in \mathbb{R}^3 with breaks along double point arcs to record the relative heights of the corresponding sheets with respect to the projection π .

By adding breaks along the double point arcs of $\pi(K)$ in this way we obtain a 3-dimensional representation of the knotted surface $K \subseteq S^4$, from which K can be recovered up to equivalence. The surface $\pi(K)$, decorated with breaks along the double point arcs in this way, is called a *broken surface diagram* of K .

Given a knotted surface K , there are a number of choices that must be made in order to obtain a broken surface diagram of K , including the choice of the projection π and the initial perturbation. Different choices will result in different broken surface diagrams for K . Despite this ambiguity, there are a collection of moves that allow us to relate any two broken surface diagrams of equivalent knotted surfaces. These seven moves are called *Roseman moves*, and they play the same role as Reidemeister moves for classical knot diagrams.

Theorem 1 (Roseman [16]) *Let K and K' be equivalent knotted surfaces in S^4 . Let D and D' be broken surface diagrams in \mathbb{R}^3 for K and K' respectively. Then the diagram D' can be converted to D by applying a sequence of Roseman moves in Figure 6, along with ambient isotopies in \mathbb{R}^3 .*

1.3 Examples of knotted surfaces

Armed with our first set of diagrammatic tools, we now proceed to define two important families of knotted surfaces: *ribbon 2-knots* and *twist/roll spun knots*.

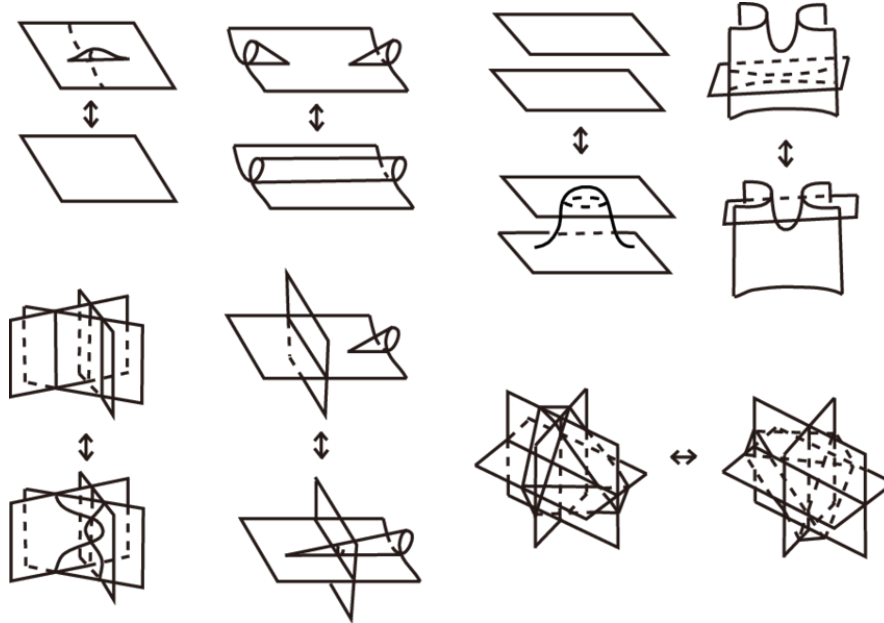


Fig. 6 Seven Roseman moves which, along with isotopy in \mathbb{R}^3 , allow us to relate the broken surface diagrams of any two equivalent knotted surfaces (see Theorem 1). Here, the breaks in the diagrams are omitted for clarity. This image was taken from the article *Showing distinctness of surface links by taking 2-dimensional braids* by Inasa Nakamura, first published in the Pacific Journal of Mathematics in Vol. 278 (2015), No. 1, published by Mathematical Sciences Publishers [14].

1.3.1 Ribbon 2-knots

To construct our first family of knotted surfaces, we start with a collection of k disjoint, unknotted 2-spheres S_1, S_2, \dots, S_k in S^4 . We also choose $k - 1$ disjoint embedded arcs $\alpha_1, \dots, \alpha_{k-1}$, each of which has its endpoints in $S_1 \cup \dots \cup S_k$, but whose interiors are disjoint from the S_j . We chose these arcs so that the union $S_1 \cup \dots \cup S_k \cup \alpha_1 \cup \dots \cup \alpha_{k-1}$ is connected.

Along the arcs $\alpha_1, \dots, \alpha_{k-1}$ we can embed a collection of disjoint 3-dimensional 1-handles h_1, \dots, h_{k-1} , which are attached to the spheres S_1, \dots, S_k . In other words, each h_j the image of an embedding $i_j : B^2 \times [0, 1] \hookrightarrow S^4$ such that $\alpha_j = i_j(\{0\} \times [0, 1])$, and $h_j \cap (S_1 \cup \dots \cup S_k) = i_j(B^2 \times \{0, 1\})$. We can surger the 2-spheres S_1, \dots, S_k along each of h_j by forming the set

$$\left(S_1 \cup \dots \cup S_k \setminus i_j(B^2 \times \{0, 1\}) \right) \cup i_j(\partial B^2 \times [0, 1]).$$

The result of surgering along each of these 1-handles h_j will be an embedded 2-sphere in S^4 (see Exercise 1.5). We call a knotted surface obtained in this way a *ribbon 2-knot*.

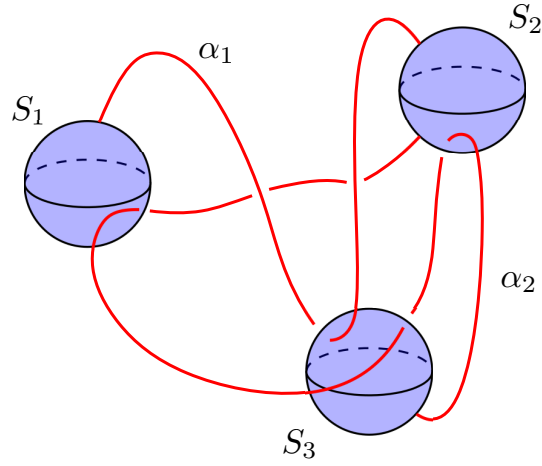


Fig. 7 A collection of disjoint, embedded, unknotted 2-spheres S_1, \dots, S_k with arcs $\alpha_1, \dots, \alpha_{k-1}$, which specify the cores of the 3-dimensional 1-handles h_1, \dots, h_{k-1} . Note that because this diagram lives in 4-space the arcs can loop through and link with the 2-spheres in nontrivial ways.

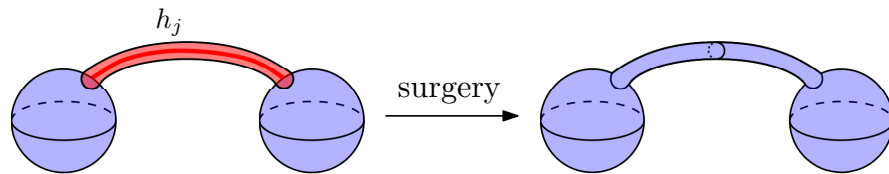


Fig. 8 Performing surgery to a pair of spheres along an embedded 3-dimensional 1-handle.

1.3.2 Twist and roll spun knots

The next family of knots we'll describe are called *spun knots*, and were originally described by Artin [3], with later enhancements described by Zeeman (*twist spun knots*) [19] and Fox (*roll spun knots*) [6]. Our description below is due to Litherland [13].

Let L be a classical knot in S^3 . By removing an open 3-ball from S^3 which intersects L in a trivial 1-stranded tangle, we obtain a 1-strand tangle pair (B^3, \mathring{L}) . Now, imagine drilling out an open tubular neighborhood $\nu(\mathring{L})$ of the tangle \mathring{L} from the 3-ball B^3 . The complement $B^3 \setminus \nu(\mathring{L})$ has a torus boundary $T = \partial(B^3 \setminus \nu(\mathring{L}))$, and along this boundary we can embed a collar neighborhood $T \times [0, 1]$. We will think of $T \cong S^1 \times S^1$, where $S^1 \times \{\text{pt}\}$ is a meridian of L , and $\{\text{pt}\} \times S^1$ is a 0-framed longitude of L . Finally, since $T \times [0, 1] \subseteq B^3 \setminus \nu(\mathring{L}) \subseteq B^3$ we will think of the thickened torus $T \times [0, 1]$ as living in B^3 and running parallel along the union $\partial B^3 \cup \mathring{L}$.

For integers m, n let $\varphi_{m,n} : B^3 \rightarrow B^3$ be a diffeomorphism defined on $T \times [0, 1] \cong S^1 \times S^1 \times [0, 1]$ by setting

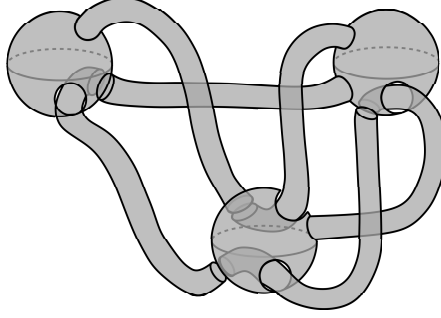


Fig. 9 A broken surface diagram of a ribbon 2-knot constructed from the arcs and spheres in Figure 7.

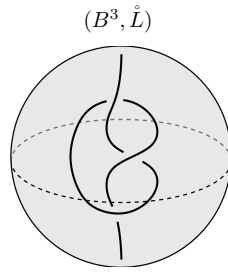


Fig. 10 A 1-strand tangle pair (B^3, \dot{L}) , obtained by removing a small 3-ball neighborhood of a point on L from S^3 .

$$\varphi_{m,n}(\theta_1, \theta_2, t) = (\theta_1 + 2\pi mt, \theta_2 + 2\pi nt, t),$$

and defined to be the identity away from $T \times [0, 1]$. Note that $\varphi_{m,n}$ serves to twist the torus T (a total of m times in the meridional direction and n times in the longitudinal direction) as we travel from 0 to 1 in the second factor of $T \times [0, 1]$.

We now take the product of the tangle pair (B^3, \dot{L}) with the interval $[0, 1]$, and glue the endpoints together via the map $\varphi_{m,n}$:

$$(B^3, \dot{L}) \times [0, 1] / (x, 0) \sim (\varphi_{m,n}(x), 1).$$

Since $\varphi_{m,n}$ is isotopic to the identity on B^3 , the resulting ambient space is diffeomorphic to $B^3 \times S^1$, while \dot{L} traces out an annulus A properly embedded in $B^3 \times S^1$. Furthermore, since $\varphi_{m,n}$ restricts to the identity on ∂B^3 , we have $\partial A = \partial \dot{L} \times S^1 \subseteq \partial B^3 \times S^1$. We can thus glue $(S^2 \times D^2, \partial \dot{L} \times D^2)$ to the pair $(B^3 \times S^1, A)$ to obtain a 2-sphere $\tau^m \rho^n(L)$ embedded in $S^4 = (B^3 \times S^1) \cup (S^2 \times D^2)$:

$$(S^4, \tau^m \rho^n(L)) := (B^3 \times S^1, A) \cup (S^2 \times D^2, \partial \dot{L} \times D^2).$$

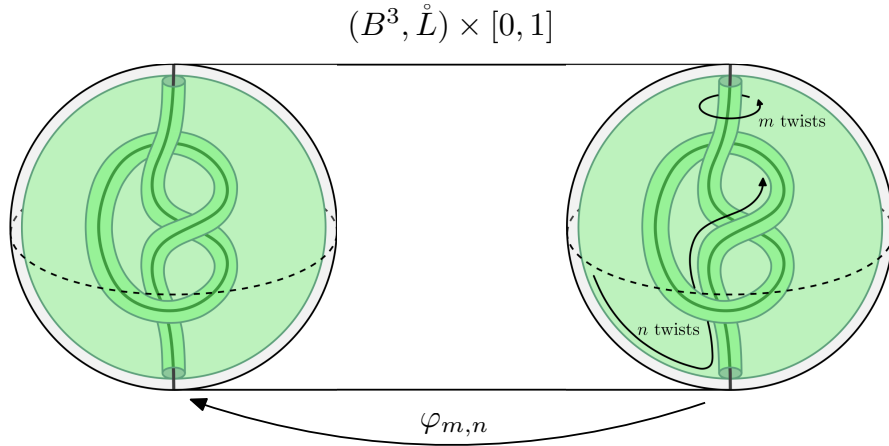


Fig. 11 Constructing a twist roll spun knot, by forming the mapping torus of a tangle pair (B^3, \mathring{L}) under the diffeomorphism $\varphi_{m,n}$. We construct a torus (in green) by taking a parallel copy of ∂B^3 , and then adding a tube that follows along the tangle \mathring{L} . The diffeomorphism $\varphi_{m,n}$ is constructed by twisting B^3 a total of m -times along a meridian of this torus, and n -times along its longitude.

We call $\tau^m \rho^n(L)$ the m -twist n -roll spin of L . Up to equivalence $\tau^m \rho^n(L)$ only depends on the choice of L . When $n = 0$ we simply call $\tau^m(L) := \tau^m \rho^0(L)$ the m -twist spin of L , while $\rho^n(L) := \tau^0 \rho^n(L)$ is called the n -roll spin of L .

A more geometric description of twist and roll spun knots can be obtained as follows [15]. Starting with the knot L , take the connected sum of L with its mirror \bar{L} . The knot $L\#\bar{L}$ bounds a disk D_L in B^4 , which can be seen by starting with a symmetric diagram of $L\#\bar{L}$, and rotating the left half of the diagram through B^4 about its axis of symmetry, ending at the right half of the diagram as in Figure 12.

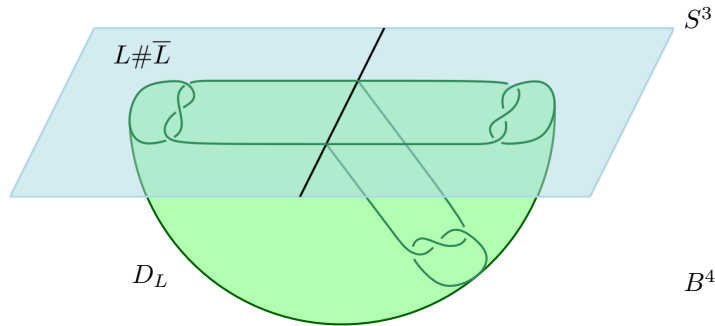


Fig. 12 A disk in B^4 bounded by $L\#\bar{L}$.

Now, let $C \subseteq S^3 \times [0, 1]$ be a concordance between $L\#\bar{L}$ and itself. In other words, C is an annulus properly embedded in $S^3 \times [0, 1]$ with $C \cap (S^3 \times \{0\}) = (L\#\bar{L}) \times \{0\}$ and $C \cap (S^3 \times \{1\}) = (L\#\bar{L}) \times \{1\}$. We may glue separate copies of the disk/ball pair (B^4, D_L) to both ends of $(S^3 \times [0, 1], C)$, by identifying $\partial(B^4, D_L) = (S^3, L\#\bar{L})$ with $(S^3 \times \{0\}, L\#\bar{L})$ and $(S^3 \times \{1\}, L\#\bar{L})$ respectively. This results in a 2-sphere Σ_C embedded in $S^4 \cong B^4 \cup (S^3 \times [0, 1]) \cup B^4$.

Different choices of concordance C will give rise to different 2-knots Σ_C . If we take C to be the trivial concordance $(L\#\bar{L}) \times [0, 1] \subseteq S^3 \times [0, 1]$ then after capping off we obtain the (0-twist, 0-roll) spun knot $\tau^0\rho^0(L)$.

We can instead modify the trivial concordance $C = (L\#\bar{L}) \times [0, 1]$ by adding m twists to one of the connect summands of $L\#\bar{L}$ as we travel up from 0 to 1 (see Figure 13). We'll denote the resulting concordance C_{τ^m} . Capping off C_{τ^m} with copies of (B^4, D_L) as above gives $\tau^m(L)$, the m -twist spin of L .

Alternatively, we can modify C by shrinking one of the connect summands of $L\#\bar{L}$, and pulling it along its strand (through the other connected summand, see again Figure 13) and back to its starting position. If we do this n times as we travel along the concordance from 0 to 1 we obtain a concordance we denote by C_{ρ^n} . By capping off C_{ρ^n} off we now obtain $\rho^n(L)$, the n -roll spin of L .

Finally, the m -twist n -roll spin $\tau^m\rho^n(L)$ is obtained by stacking the two concordances C_{τ^m} and C_{ρ^n} together, before capping the resulting concordance off as before.

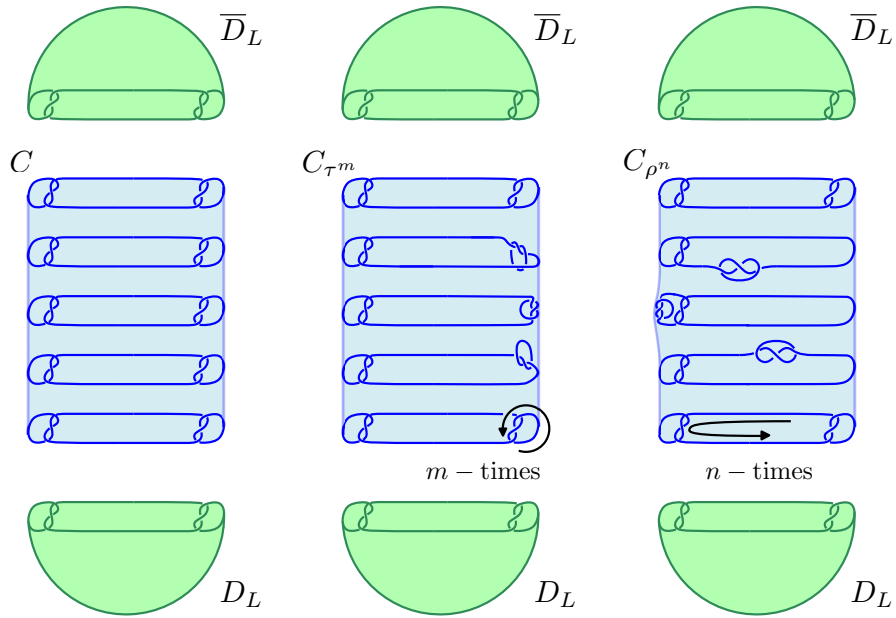
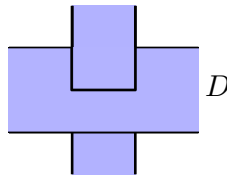


Fig. 13 Building twist roll spun knots by capping off concordances with ribbon disks.

Exercises

- 1.1. Show that the two knotted surfaces in Figure 3 are equivalent.
- 1.2. Consider a spun trefoil knot K . How would you draw a broken surface diagram for K ? (It may be difficult to actually draw it, but give it a shot.)
- 1.3. Show that the 0-twist 0-roll spun left-handed trefoil is isotopic to the 0-twist 0-roll spun right-handed trefoil. (*Hint: You'll need to think carefully about the orientation of the ambient space here.*) Does your proof still work if you consider an n -twist spun trefoil?
- 1.4. Let K be an orientable surface knot, and let S^3 denote the standard 3-sphere lying in S^4 . Show that if K bounds a 3-dimensional handlebody then K can be isotoped to lie entirely in $S^3 \subseteq S^4$. Can you prove the converse? (It's true, but more difficult to prove.)
- 1.5. Prove that the result of performing surgery along a connected complex of k embedded 2-spheres S_1, \dots, S_k and $k - 1$ arcs $\alpha_1, \dots, \alpha_{k-1}$ as described in Section 1.3.1 is orientable, and is an embedded 2-sphere.
- 1.6. A *ribbon disk* $D \subseteq S^3$ is an immersed disk with only ribbon intersections, i.e. intersections of the form shown below:



A (*classical*) *ribbon knot* $J \subseteq S^3$ is a knot which arises as the boundary of a ribbon disk. Any ribbon disk can be pushed slightly into B^4 to yield a properly embedded disk which does not have any local maxima with respect to the radial distance function on B^4 . (Here, we think of S^3 as the boundary of B^4 .)

- a. Show that any ribbon 2-knot in S^4 can be isotoped so that its intersection with the equatorial 3-sphere is a classical ribbon knot.
 - b. In the above situation, does the ribbon knot $J = S^3 \cap K$ depend only on the 2-knot K ? If not, how do the choices we make affect J ?
 - c. Show that any ribbon 2-knot K in S^4 can be obtained as the double of an embedded ribbon disk $D \subseteq B^4$. In other words, (S^4, K) can be obtained by gluing two copies of (B^4, D) together via the identity along $S^3 = \partial B^4$.
- 1.7. Let L be an m -component unlink in S^3 , and let E and E' each be a set of m disks smoothly embedded in S^3 whose boundaries are the unlink L . Show that E and E' are smoothly isotopic rel boundary in B^4 . In other words, after pushing the interiors of E and E' slightly into B^4 , show that there is an isotopy which takes E to E' , fixing their boundaries. (*Hint: Try to work out the $m = 1$ case first. You'll probably want to invoke the 3-dimensional Schoenflies theorem here, which states that any smoothly embedded 2-sphere in S^3 bounds a smoothly embedded 3-ball.*)

2 Banded unlink diagrams of knotted surfaces and Swenton's theorem

Although broken surface diagrams are useful for representing knotted surfaces in S^4 , they can be difficult to draw and somewhat cumbersome to work with, especially for particularly complicated surfaces. In this section we discuss banded unlink diagrams, which allow us to represent surfaces via a single diagram of a classical (1-dimensional) link with bands attached. In addition to being easier to draw, they also have the advantage of generalizing to surfaces in arbitrary smooth 4-manifolds, which we discuss in Section 3.

2.1 Motion picture diagrams

We begin by outlining a natural technique for describing knotted surfaces in S^4 , using *motion picture diagrams*. It will be convenient to think of our knotted surfaces as living in a punctured 4-sphere, $S^4 \setminus \{\text{pt}\} \cong \mathbb{R}^4 \cong \mathbb{R}^3 \times \mathbb{R}$, where we think of the last \mathbb{R} factor in the product as describing a time coordinate. Now, given a knotted surface K for each $t \in \mathbb{R}$ we define

$$K_t = K \cap (\mathbb{R}^3 \times \{t\}).$$

We think of the set $\{K_t\}_{t \in \mathbb{R}}$ as being a family of cross-sections of our surface K , and we call the set $\{K_t\}_{t \in \mathbb{R}}$ a *motion picture* of K . Taken together, these cross-sections (called *stills* or *frames* of the motion picture) allow us to perfectly reconstruct the knotted surface K .

In general, these cross-sections K_t may be complicated. However, after an arbitrarily small perturbation we may arrange K so that the projection $\pi : \mathbb{R}^3 \times \mathbb{R} \rightarrow \mathbb{R}$ restricts to a Morse function on K , where each $t \in \mathbb{R}$ is the image of at most one critical point of $\pi|_K$. In this situation K_t will be a link in $\mathbb{R}^3 \times \{t\} \cong \mathbb{R}^3$ for all but finitely many t (which correspond to the critical values of the Morse function $\pi|_K$).

When $t \in \mathbb{R}$ is a critical value of $\pi|_K$ the set K_t will be a singular link in \mathbb{R}^3 , with singular points corresponding to either relative minima, relative maxima, or saddle points of the Morse function $\pi|_K$. Thus, for nearby regular values $t, t' \in \mathbb{R}$, the links K_t and $K_{t'}$ will differ by one of the following (see Figure 15):

1. the deletion of an unknotted component, if $[t, t']$ contains a local maximum,
2. two strands recombining, if $[t, t']$ contains a saddle point,
3. the addition of an unknotted component, if $[t, t']$ contains a local minimum, or
4. an ambient isotopy, if $[t, t']$ contains only regular values.

In practice, we don't need to keep track of the infinite family of cross-sections $\{K_t\}_{t \in \mathbb{R}}$. Instead, we only need to record a finite sequence $K_{t_0}, K_{t_1}, \dots, K_{t_N}$ of cross-sections for some regular values $t_0 < t_1 < \dots < t_N$. We represent these cross-sections as a sequence of link diagrams $D_{t_0}, D_{t_1}, \dots, D_{t_N}$. In order to preserve

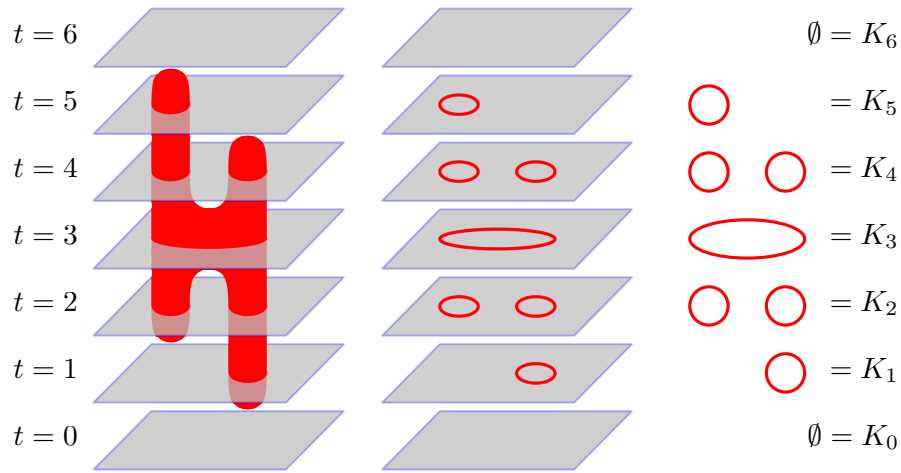


Fig. 14 Representing a surface by a sequence of cross-sections. Notice that this figure depicts a surface in 3-space, and hence all of the nonsingular cross-sections are unlinks. For knotted surfaces in 4-space, the level sets K_t will in general be knotted.

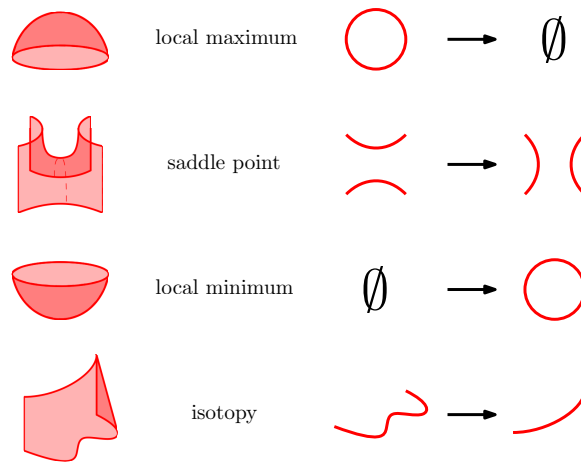


Fig. 15 Nearby regular values t and t' of $\pi|_K$ will give rise to level sets K_t and $K_{t'}$, which differ by one of the above modifications, corresponding to passing a Morse critical point (local maximum, saddle point, or local minimum), or ambient isotopy if the interval $[t, t']$ doesn't contain any critical values.

enough information to accurately recover the surface K , we need enough t_j values so that when reconstructing K it is clearly evident how to interpolate between adjacent cross-sections K_{t_j} and $K_{t_{j-1}}$, whether it be by a single Morse critical point or a specific isotopy. (Choosing a different isotopy taking $K_{t_{j-1}}$ to K_{t_j} may result in inequivalent knotted surfaces after reconstructing.) To accomplish this, the t_j values are often

chosen so that each pair of adjacent diagrams D_{t_j} and $D_{t_{j-1}}$ differ by either a single Reidemeister move, Morse critical point, or simple planar isotopy. The family of diagrams $\{D_{t_0}, D_{t_1}, \dots, D_{t_N}\}$ is called a *motion picture diagram* of K .

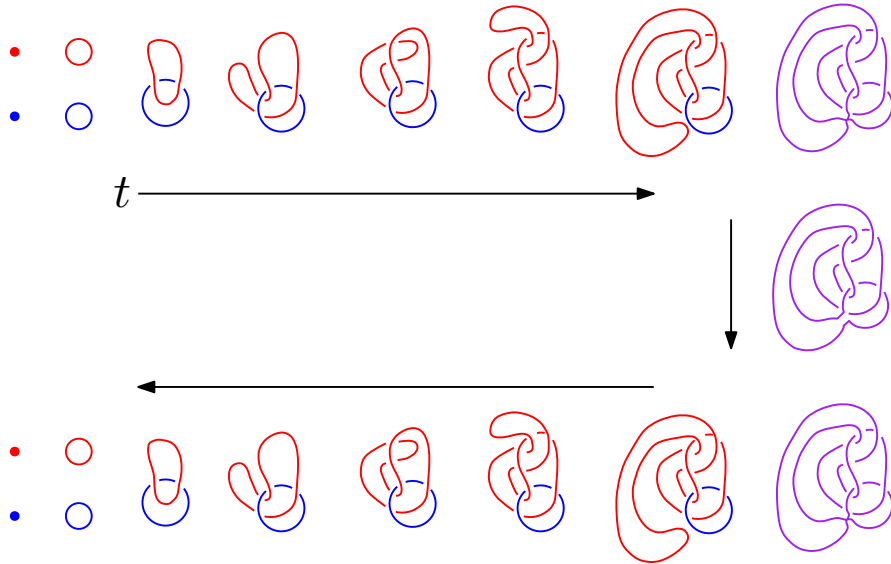


Fig. 16 A motion picture diagram of a knotted sphere, with two (global) minima, two saddle points, and two (global) maxima. In this figure we illustrate the singular level sets for clarity, though they are often omitted from the motion picture.

2.2 Banded unlink diagrams

Motion picture diagrams are easy to interpret, though the sequences of frames needed to adequately describe complicated surfaces can still be quite long. In this section we will see how all of the important topological information contained in a motion picture diagram can be expressed in a single frame of the diagram, significantly reducing the number of diagrams that need to be drawn.

The first step will be to “flatten” a small neighborhood of each critical point of the surface K . By applying an isotopy supported in a small neighborhood of each critical point, we can flatten the local maxima, local minima, and saddle points to obtain *minimum disks*, *maximum disks*, and *saddle bands* as in Figure 17. The motion picture in Figure 18 shows the result of flattening the critical points in the knotted surface defined in Figure 16.

Notice that passing a minimum disk in our surface results in a new unknotted component appearing in the subsequent cross-sections of the motion picture. Passing

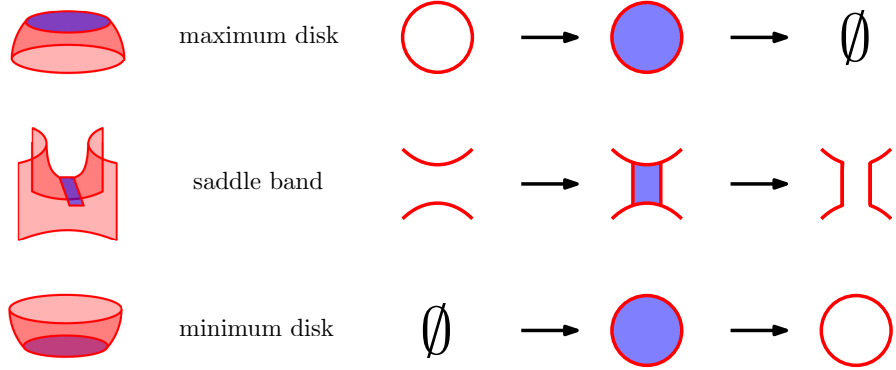


Fig. 17 By applying a small isotopy in a neighborhood of each critical point we can flatten out the local minima, local maxima, and saddle points to obtain minimum disks, maximum disks, and saddle bands respectively.

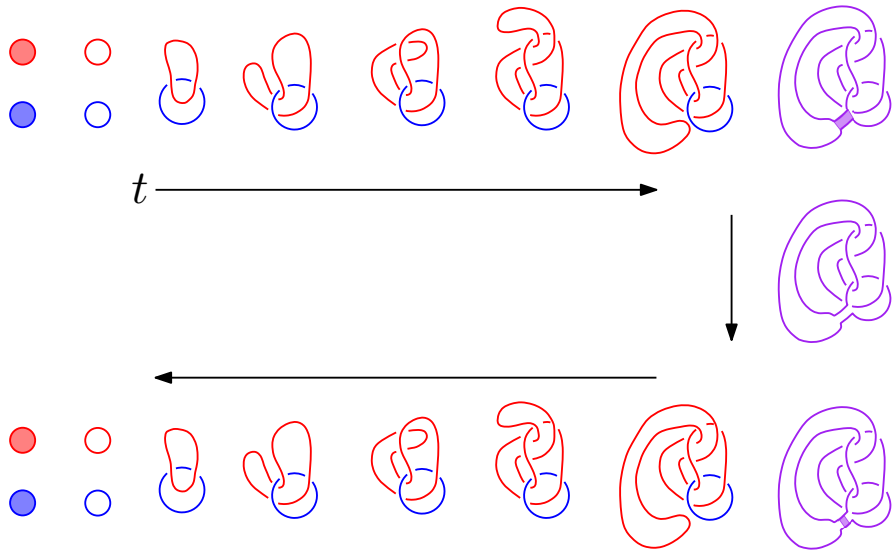


Fig. 18 The knotted surface from Figure 16, with critical points flattened.

a maximum disk likewise removes an unknotted component from appearing in the subsequent cross-sections. When passing a saddle band the cross-sections of K change by a band surgery, as in Figure 19. In fact, it will be convenient to establish some notation here for what follows. Suppose that L is a link in S^3 , and that B is a collection of bands attached along L . Then the result of performing surgery to L along the bands B is denoted by L_B (see Figure 20).

Returning to our example, note that the representation of the surface in Figure 18 can be simplified further, by elongating the saddle bands and stretching out the

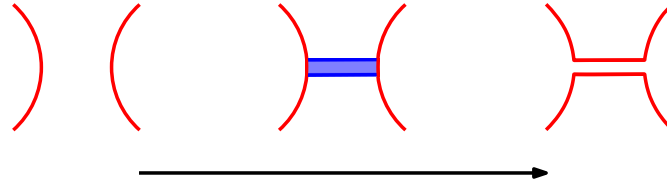


Fig. 19 The effect of passing a saddle band in a motion picture with flattened critical points.

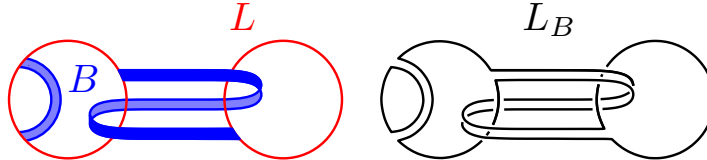


Fig. 20 Performing surgery to a link L along bands B , resulting in a new link L_B .

maximum disks. Indeed, much of the diagram in Figure 18 is dedicated to describing the isotopies of the two circles that are created by the pair of minima, as well as the pair of circles that disappear at the maxima. Instead of isotoping the circles around shortly after they are created, we can isotope the surface so that the circles stay in a fixed position after they appear. To compensate for fixing the circles, the saddle bands must be stretched along the path of the isotopy of the circles from the original diagram. Similarly, if we want to keep the circles fixed after the saddle bands we can do so, at the expense of stretching the maximal disks to compensate. These modifications are illustrated in Figure 21, which represents the same surface as in Figures 16 and 18.

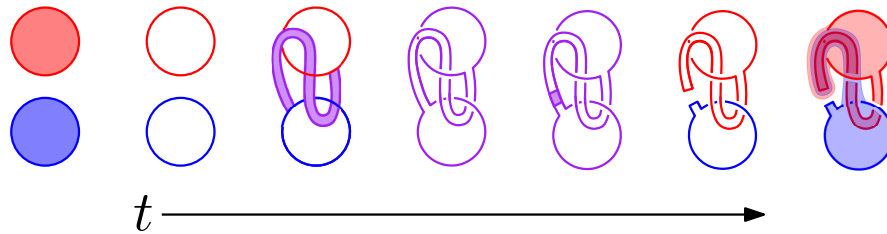


Fig. 21 The knotted surface from Figures 16 and 18, where we have fixed the position of the circles that appear from the minimum disks by lengthening the bands and stretching the maximum disks accordingly.

Notice that in the surfaces we have drawn so far, the critical points have all been ordered so that the minimal disks occur first, followed by the saddle bands, and finally the maximal disks. While this won't be the case with every knotted surface

that you encounter in the wild, the following useful fact can be used to exchange the relative heights of critical points to achieve this:

Lemma 1 *Given a knotted surface $K \subseteq \mathbb{R}^4$ represented by a motion picture diagram with flattened critical points as above, the following rearrangements can always be achieved by an ambient isotopy:*

1. a maximum disk can be pushed above any other critical point,
2. a minimum disk can be pushed below any other critical point,
3. the relative heights of two saddle bands can be interchanged, and
4. a saddle band can be pushed above any minimal disk, or below any maximal disk.

Notice that Lemma 1 does not allow us to push a saddle band below a minimum disk or above a maximum disk. This will not be possible if the saddle band of interest is attached to the circle that is created by the minimum disk, for example. See Figure 22 for an illustration of Lemma 1. Notice that in Figure 22 the saddle bands can be kept disjoint while their heights are exchanged. This won't always be the case, as we will see below.

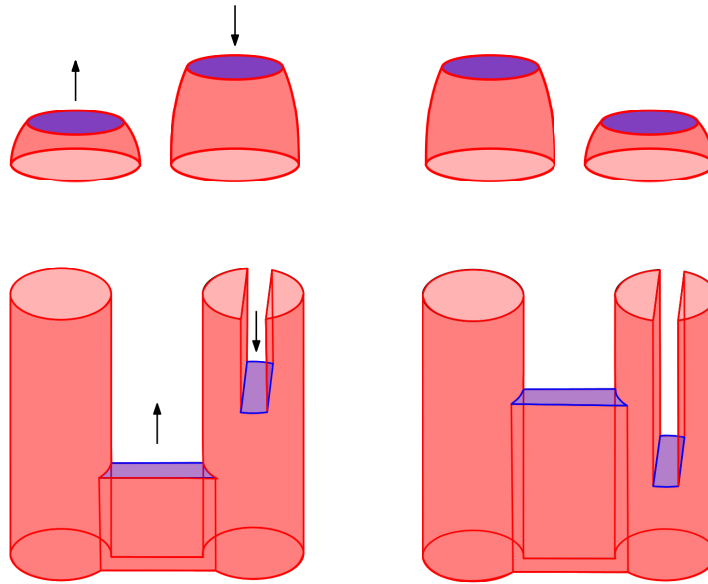


Fig. 22 The relative heights of a pair of maximum disks is exchanged, as well as the relative heights of two saddle bands. See Lemma 1 for a more detailed description of when the heights of two critical points may be exchanged.

By repeated application of Lemma 1 to our knotted surface K , we can actually arrange something stronger:

Proposition 1 *After ambient isotopy, K can be arranged with respect to the height function on $\mathbb{R}^4 \cong \mathbb{R}^3 \times \mathbb{R}$ such that*

1. *all minimum disks lie in $\mathbb{R}^3 \times \{-1\}$,*
2. *all saddle bands lie in $\mathbb{R}^3 \times \{0\}$, and*
3. *all maximum disks lie in $\mathbb{R}^3 \times \{1\}$.*

For a surface arranged as in Proposition 1 all of the important information about the surface is contained in $K_0 = K \cap (\mathbb{R}^3 \times \{0\})$ (see Figure 23). In fact, once the central cross-section K_0 is fixed, the minimum and maximum disks are uniquely determined up to isotopy in $\mathbb{R}^3 \times (-\infty, -1]$ and $\mathbb{R}^3 \times [1, \infty)$ respectively (see Exercise 1.7). Thus, up to ambient isotopy the knotted surface K can be entirely described by the central cross-section K_0 .

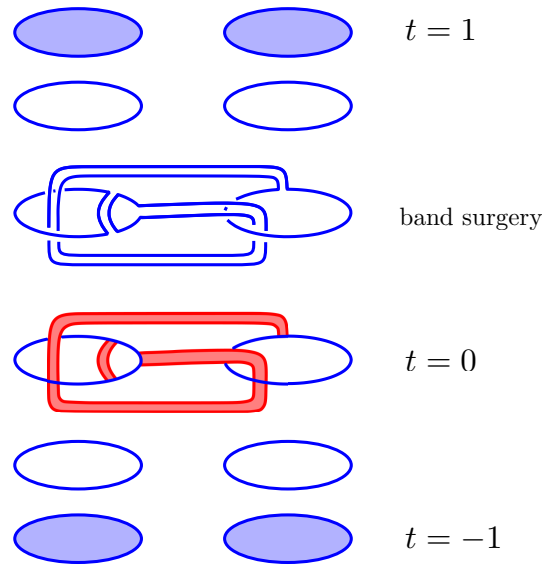


Fig. 23 A knotted surface whose minimum disks, saddle bands, and maximum disks are arranged as in Proposition 1.

Note that for a knotted surface K as in Proposition 1, the central cross-section K_0 will consist of a link L with a collection of bands B attached. Since the link L was created as the boundaries of disjoint minimal disks at height $t = -1$, the link L will necessarily be an unlink. Furthermore, since K must be capped off with maximal disks at height $t = 1$, we necessarily end up with an unlink after performing the band surgeries along the bands in B . In other words, the cross-section K_0 must consist of an unlink L , together with a set of bands B such that L_B is also an unlink. This motivates the following definition:

Definition 5 *A banded unlink diagram is a pair (L, B) , where*

1. L is an unlink in \mathbb{R}^3 ,
2. B is a finite collection of bands attached along L , and
3. L_B is an unlink in \mathbb{R}^3 .

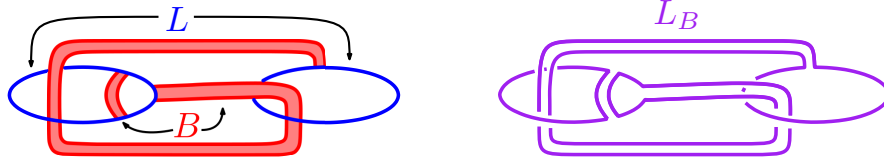


Fig. 24 Left: An unlink L with bands B attached. Right: Since the result of performing band surgery to L along B is again an unlink, the pair (L, B) is a banded unlink diagram.

Given a banded unlink diagram $(L, B) \subseteq \mathbb{R}^3$, we obtain a knotted surface $\Sigma(L, B)$ in \mathbb{R}^4 as follows. First, we view (L, B) as living in $\mathbb{R}^3 \times \{0\} \subseteq \mathbb{R}^4$, and we cap off L with boundary parallel disks embedded in $\mathbb{R}^3 \times (-\infty, 0]$, and cap off L_B with boundary parallel disks embedded in $\mathbb{R}^3 \times [0, \infty)$ as in Figure 25. Because these embedded disks are unique up to isotopy rel boundary, the resulting surface $\Sigma(L, B)$ is well-defined up to isotopy.

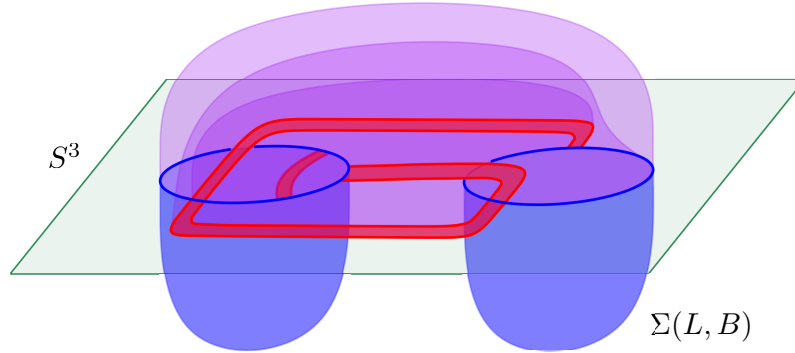


Fig. 25 Building a knotted surface $\Sigma(L, B) \subseteq \mathbb{R}^4$ from a banded unlink diagram (L, B) in $\mathbb{R}^3 \times \{0\}$. Embedded disks are used to cap off the unlink L from below, and the unlink L_B from above.

Theorem 2 *If $(L, B) \subseteq \mathbb{R}^3$ is a banded unlink diagram, then the surface $\Sigma(L, B) \subseteq \mathbb{R}^4$ obtained from capping off L and L_B with boundary parallel disks as described above is unique up to isotopy.*

In light of Theorem 2, once we've positioned all of the saddle bands at height $t = 0$ we can represent a knotted surface K via the banded unlink at its central

cross-section K_0 . This gives us a compact way of representing knotted surfaces in \mathbb{R}^4 and S^4 .

It's worth noting that banded unlink diagrams are related to another technique of representing knotted surfaces called *normal forms*. For surfaces in normal form the saddle bands are separated between two different levels, while the cross sections in between are connected. See [2, 11], for example, for more details.

2.3 Swenton's theorem

Now that we've seen how knotted surfaces gives rise to banded unlink diagrams and vice versa, it's worth asking to what extent a knotted surface uniquely determines a banded unlink diagram. To see this, it's instructive to try converting a motion picture diagram to a banded unlink diagram.

Consider again the motion picture in Figure 21. Because the second band is attached along segments of the link that were created by the first band surgery, directly pushing the two bands to the same level will result in intersections between the bands. To avoid this, we may slide the second band along the link slightly, so that it avoids the other band when the two bands are pushed to the same level (see Figure 26).

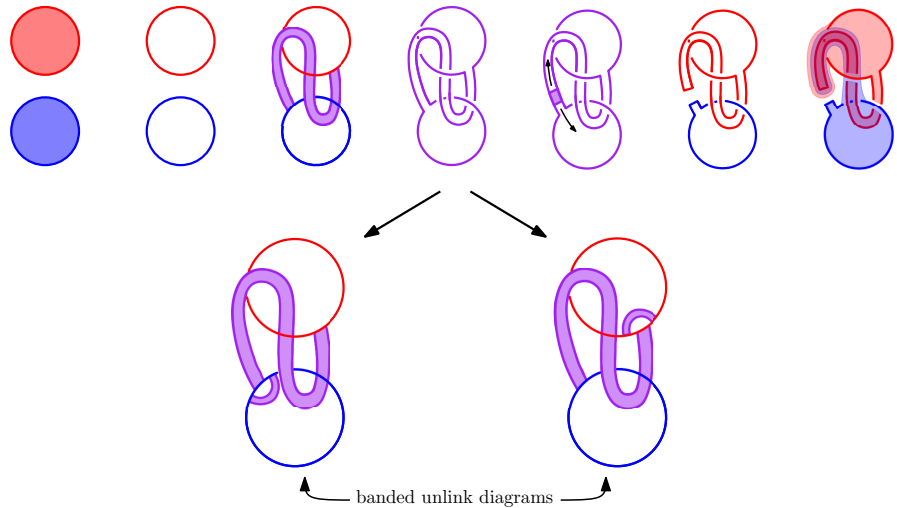


Fig. 26 Converting a motion picture diagram to a banded unlink diagram. This requires sliding one of the bands out of the way of the other band so that they can be pushed to the same level. The choice of which direction to push the band will result in banded unlink diagrams that differ by a sequence of band slides as illustrated in Figures 28 and 29.

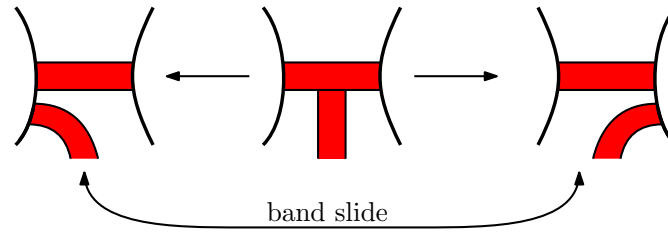


Fig. 27 If the endpoint of one band intersects the edge of a different band when pushed to the same level then the intersection can be resolved in one of two ways. The resulting banded unlink diagrams will differ by a band slide operation.

Note, however, that there were two directions we could have slid the band (or, we could have slid one end of the band one direction, and the other end of the band in the other direction). Sliding the band in the other direction would have resulted in a different banded unlink diagram for the same knotted surface. The resulting two banded unlink diagrams will differ from each other by a sequence of *band slides*, where the endpoint of one band is dragged along the edge of another band as in Figure 28.

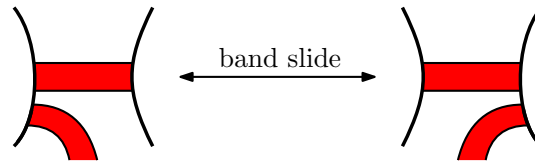


Fig. 28 A band slide operation, which changes the banded unlink diagram but does not change the isotopy class of the resulting surface.

Alternatively, a motion picture of K may involve a pair of bands which (if pushed to the same level) would intersect in the interior of one band as in Figure 30. Avoiding such self-intersections requires choosing a direction to push the band out of the way, and the choice of pushing direction results in banded unlink diagrams that differ by a band swim operation, illustrated in Figure 31.

The band slide and band swim moves are sufficient to capture the choices required when converting a given motion picture diagram into a banded unlink diagram. It is also possible, however, for different motion picture representations of the same surface to have different critical points under the Morse height function. For example, via a local isotopy we can always create a pair of canceling critical points, consisting of a saddle point and either a local minimum or local maximum point. When converted to the language of banded unlink diagrams, adding these pairs of canceling critical points correspond to *cap* and *cup* moves as illustrated in Figure 32.

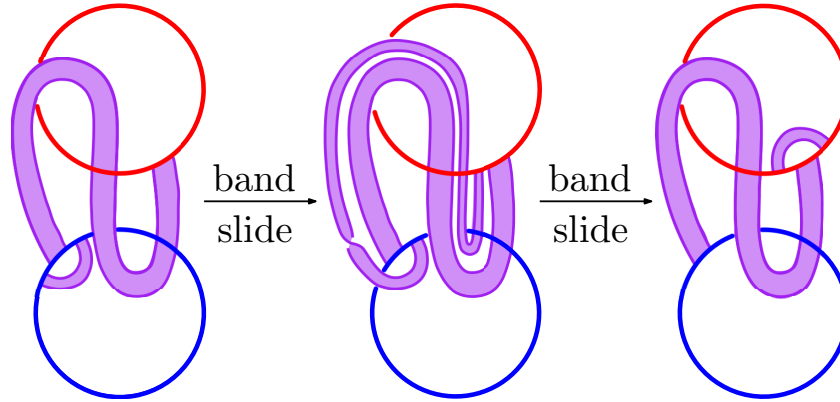


Fig. 29 A pair of band slides allows us to relate the two banded unlink diagrams of the surface depicted in Figure 26. We first slide the left endpoint of the smaller band along the edge of the larger band, before sliding the right endpoint of the smaller band along the larger band. Notice that the band has a half-twist after the first slide, which is undone by the second slide.

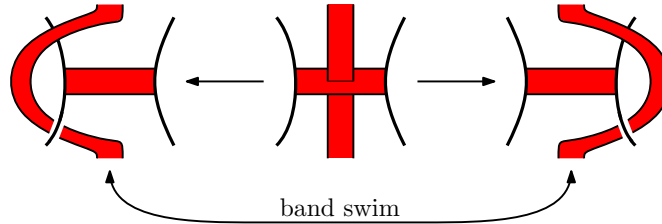


Fig. 30 There are two ways of pushing a band out of the way to avoid intersections in the interior of a band. The resulting pair of diagrams differ by a band swim as illustrated in Figure 31.

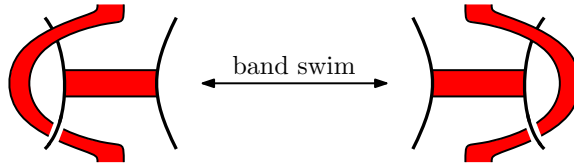


Fig. 31 A band swim operation, which changes the banded unlink diagram but does not change the isotopy class of the resulting surface.

The following theorem establishes that the above moves are sufficient to relate the banded unlink diagrams of any two isotopic knotted surfaces. It was originally conjectured by Yoshikawa [18] and was proved by Swenton, with an alternate proof being given by Kearton and Kurlin. We won't discuss the proof here, but will outline the proof of a generalized version of this theorem in Section 3.

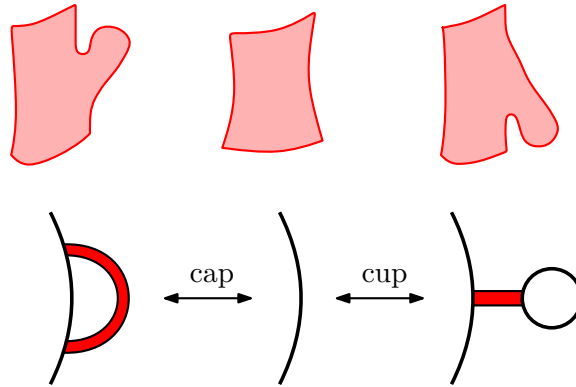
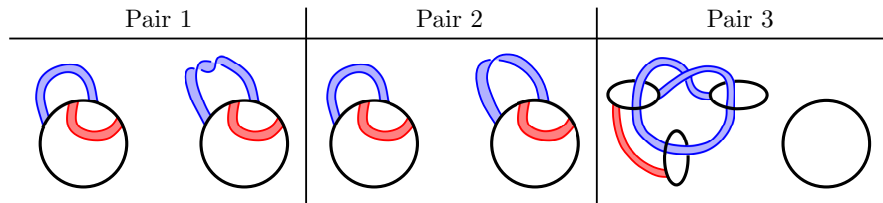


Fig. 32 The cap and cup moves, each of which correspond to adding/removing pairs of canceling critical points.

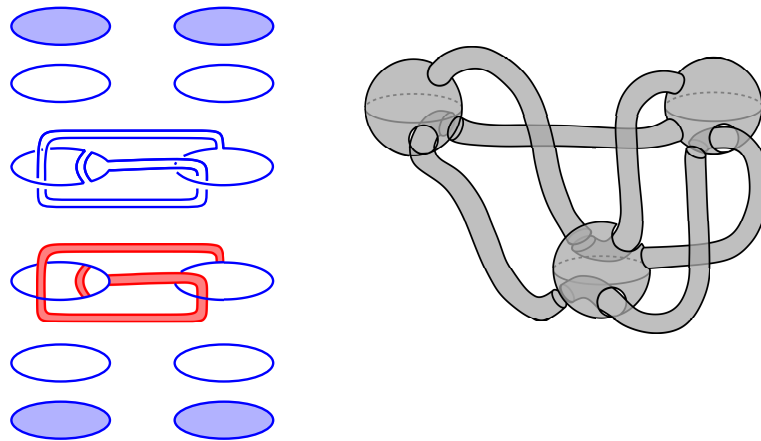
Theorem 3 (Swenton [17], Kearton-Kurlin [12]) *Let (L, B) and (L', B') be banded unlink diagrams. Then the knotted surfaces $\Sigma(L, B)$ and $\Sigma(L', B')$ are isotopic in \mathbb{R}^4 if and only if (L, B) and (L', B') can be joined by a sequence of band slides, band swims, cap and cup moves, and isotopy in \mathbb{R}^3 .*

Exercises

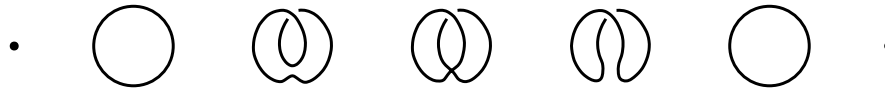
- 2.1. For the following pairs of banded unlink diagrams, try to determine which pairs determine isotopic surfaces. Can you identify the underlying surfaces? (*Hint: Try to find band slides/swims to convert one diagram to the other if you can, or find a reason why no such sequence of moves exists.*)



- 2.2. Convert both the motion picture diagram and broken surface diagram below to banded unlink diagrams. Can you convert the broken surface diagram to a motion picture diagram, and vice versa?

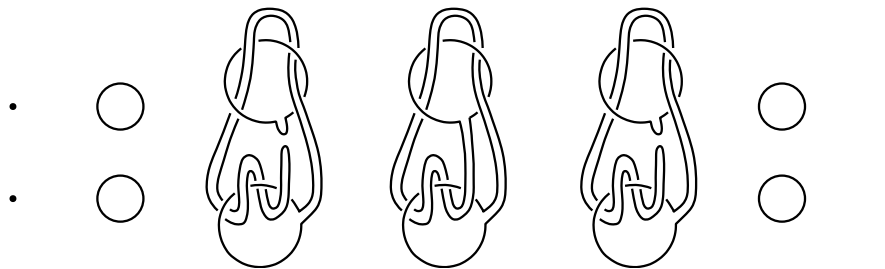


2.3. A projective plane in S^4 is said to be *unknotted* if it is isotopic to the surface P_0 below or its mirror (the figure below has a single saddle point in the central frame):



A nonorientable surface in S^4 is said to be *unknotted* if it is isotopic to a connected sum of a finite number of unknotted $\mathbb{R}P^2$ in S^4 .

- a. Starting from the motion picture above, draw a banded unlink diagram of P_0 .
- b. Draw a banded unlink diagram of the ribbon 2-knot K below:



- c. Show that the connected sum of the above 2-knot K and P_0 is another unknotted $\mathbb{R}P^2$. In other words, $K\#P_0 = P_0$.

This example is due to Viro. It can be shown that K is knotted by looking at $\pi_1(S^4 \setminus K)$. It shows that unlike in the classical dimension, unknotted surfaces may remain unknotted, even after taking connected sums with knotted surfaces.

- 2.4. a. Draw a banded unlink diagram of the spun trefoil. (*Hint: Start by drawing a symmetric diagram of the connected sum of the trefoil with its mirror. Think of this as the middle cross-section of the spun knot, so half of the spinning takes place above the plane of the diagram and the other half takes place below it. Can you identify which parts of the diagram will contribute min/max disks when spun? And where the saddle bands will appear? As an extra hint, notice that the bands will appear in pairs, each pair contributing one band above the plane of the diagram and one band below it.*)
- b. Can you generalize your approach in part (a) to find an algorithm for producing a banded unlink diagram of any spun knot? What will determine the number of link components, and the number of bands?
- 2.5. a. Draw a banded unlink diagram of the 1-twist spun trefoil. (*Hint: Start with the diagram of the spun trefoil you drew in Exercise 2.4. Separate each pair of bands in your diagram, pushing one band above the level of the plane and one band below it. Then keep track of what will happen to these bands as you apply the twisting above plane.*)
- b. How will the result in part (a) change if you add n twists? Or if you apply it to an arbitrary knot?
- 2.6. (*Challenging Problem/Bonus Question*) In 1965 Zeeman proved that the 1-twist spin of any knot in S^3 is unknotted. (More precisely, he proved that the n -twist spin of a knot J is a fibered 2-knot, whose fiber is the punctured n -fold cyclic covering of S^3 branched over J .) Using band moves and the diagram you obtained in Exercise 2.5, show directly that the 1-twist spun trefoil is unknotted.

3 Banded unlink diagrams in arbitrary 4-manifolds

The previous methods we discussed for representing knotted surfaces (broken surface diagrams, motion picture diagrams, and banded unlink diagrams) all work well for describing surfaces in S^4 or \mathbb{R}^4 . Working with surfaces in arbitrary smooth 4-manifolds requires additional work, however. In this section we focus on generalizing the notion of banded unlink diagrams to closed surfaces smoothly embedded in arbitrary smooth 4-manifolds.

3.1 Kirby diagrams and handle decompositions of smooth 4-manifolds

One important ingredient when defining and working with banded unlink diagrams in \mathbb{R}^4 was the height function, which we took to be the restriction of the standard projection $\pi : \mathbb{R}^4 \cong \mathbb{R}^3 \times \mathbb{R} \rightarrow \mathbb{R}$. We used this height function to describe surfaces in terms of minimum disks, maximum disks, and saddle bands. We also used this height function (implicitly) to “push” the saddle bands around vertically, so that they could all be arranged in the central cross-section of the surface.

Consider now the situation when we want to describe a knotted surface which is smoothly embedded in a smooth closed 4-manifold. If we wish to describe the surface again terms of minimum disks, maximum disks, and saddle bands we need to define a height function on the ambient space. Ideally, this height function would be encoded in a way which allows us to easily understand how the knotted surface interacts with the topology of the ambient manifold. Fortunately for us, 4-manifolds are often described and studied via handle decompositions which are induced by Morse functions, and these Morse functions can be used to simultaneously describe both the embedded surface and the ambient 4-manifold.

Let X be a closed (compact, without boundary) connected smooth 4-manifold. Let $h : X \rightarrow \mathbb{R}$ be a self-indexing Morse function. In other words, h is a Morse function on X with the property that every critical point p with index i has $h(p) = i$ (every Morse function can be homotoped through Morse functions to a self-indexing one).

Recall that a Morse function $h : X \rightarrow \mathbb{R}$ induces a decomposition of X into handles. A *4-dimensional k -handle* is a space which is diffeomorphic to $B^k \times B^{4-k}$, and which is attached to a 4-manifold Y via an embedding

$$\psi : (\partial B^k) \times B^{4-k} \rightarrow \partial Y$$

which defines a gluing map for $Y \cup_{\psi} (B^k \times B^{4-k})$. The set $(\partial B^k) \times B^{4-k}$ is called the *attaching region* of the handle. The set $B^k \times \{0\}$ is called the *core* of the handle, while $\{0\} \times B^{4-k}$ is called its *cocore*.

For example, a 4-dimensional 0-handle is simply a copy of B^4 , which has an empty attaching region, and hence is “attached” to Y as a disjoint union. A 4-dimensional 1-handle is diffeomorphic to $B^1 \times B^3$, which is attached to Y by an embedding of $\partial B^1 \times B^3 = \{-1, 1\} \times B^3$ into ∂Y . In other words, we simply specify where the “feet” of the 1-handle are to be attached in ∂Y . A 4-dimensional 2-handle is diffeomorphic to $B^2 \times B^2$, which is attached to Y by an embedding of $\partial B^2 \times B^2 = S^1 \times B^2$ in ∂Y . See Figure 33 for an illustration of 4-dimensional 0-, 1-, and 2-handles, and their attaching regions.

A *handle decomposition* on X is a decomposition of $X = h_1 \cup h_2 \cup \dots \cup h_{\ell}$ into handles $\{h_1, h_2, \dots, h_{\ell}\}$, such that the handles h_j all have pairwise disjoint interiors, and each h_j is attached to $h_1 \cup h_2 \cup \dots \cup h_{j-1}$ as described above. A Morse function $h : X \rightarrow \mathbb{R}$ induces a handle decomposition of X , with one 4-dimensional k -handle for each Morse critical point of index k . If h is self-indexing, then this handle decomposition is build by first attaching the 0-handles, then attaching the 1-handles, then 2-handles, and so on, where each k -handle can be assumed to be attached to the union of the handles of index $< k$.

Conveniently, it turns out that if X is connected then we may assume that it has precisely one 0-handle B^4 . Futhermore, if X is a closed 4-manifold, then there is a unique way to glue in the 3- and 4-handles once the 0-, 1-, and 2-handles are attached. Thus to describe a handle decomposition of a closed, connected, smooth 4-manifold X , it suffices to specify how the 1- and 2-handles are attached to the boundary S^3

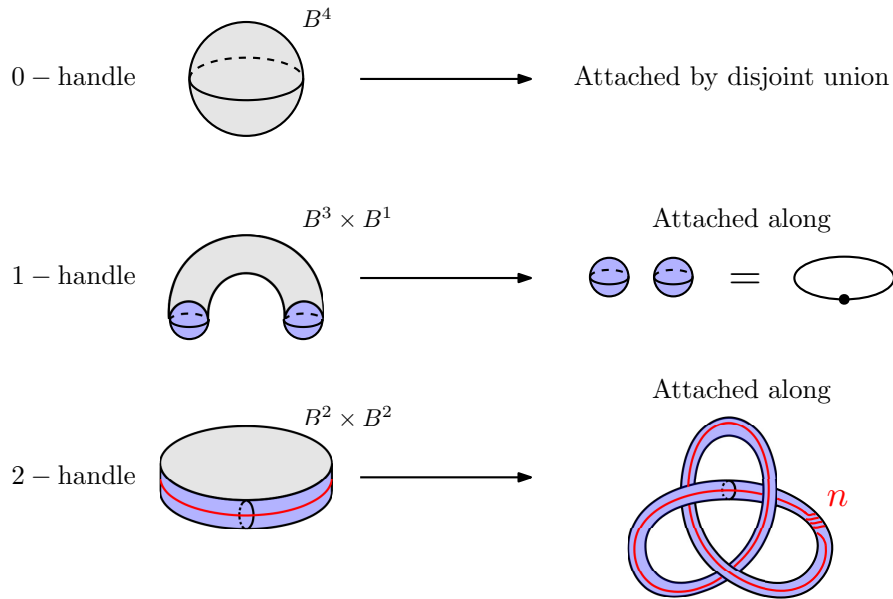


Fig. 33 Illustrations of 4-dimensional 0-, 1-, and 2-handles, along with their attaching regions (in blue). In Kirby diagrams 1-handles are specified by a pair of embedded 3-balls (the “feet” of the 1-handle), or equivalently by a dotted unknotted circle. On the other hand, 2-handle attachments are specified by framed circles, which determine embeddings of the individual handle attaching regions $S^1 \times B^2$.

of the unique 0-handle of X . These 1- and 2-handle attachments are described by a Kirby or *handlebody diagram* of X .

Each 1-handle attachment is specified by a pair of embedded 3-balls in S^3 , or equivalently, a dotted unknotted circle. (Adding a 1-handle is equivalent to deleting a 2-handle from inside the 0-handle B^4 , and this dotted circle specifies the boundary of the 2-handle that is to be deleted.)

Once the 1-handles attachments are drawn in S^3 , the 2-handles are then specified as a link in the complement of the 1-handle components, where each 2-handle link component is assigned an integer framing. The 2-handles are attached along a tubular neighborhood of this link, where the integer framing determines how each 2-handle attaching region twists along the embedding. More precisely, a 2-handle attaching circle C with framing n indicates that the attaching region $S^1 \times B^2$ is to be glued in such a way that $S^1 \times \{0\}$ is sent to C , while $S^1 \times \{1\}$ is sent to a curve that is a parallel push-off of C , but which represents the class $n \in H_1(S^3 \setminus C) \cong \mathbb{Z}$.

See Figure 34 for an example of a Kirby diagram of a closed, connected 4-manifold. For much more thorough treatments of 4-manifolds and Kirby diagrams, see [1] or [7].

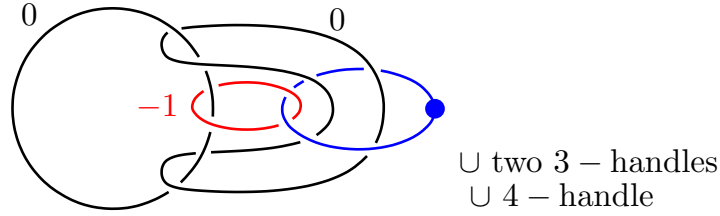


Fig. 34 A Kirby diagram of a closed, connected 4-manifold X . This diagram takes place in S^3 , which is thought of as the boundary of the unique 0-handle of X . It contains one 1-handle (represented by the dotted circle) and three 2-handles (represented by the link components with framings specified). Attaching two 3-handle and a single 4-handle (whose gluing maps are uniquely determined) caps off the handle decomposition to give a closed 4-manifold.

3.2 Banded unlink diagrams in arbitrary 4-manifolds

Now, if $h : X \rightarrow \mathbb{R}$ is a self-indexing Morse function on X , let \mathcal{K} be a Kirby diagram for the handle decomposition induced on X by h . We think of \mathcal{K} as being a link in S^3 , where each component of \mathcal{K} is decorated with either a dot and is unknotted (corresponding to a 1-handle attachment), or an integer framing (corresponding to a 2-handle attachment).

For each $t \in \mathbb{R}$, we set $M_t := h^{-1}(t)$. We can think of M_t as being the boundary of $h^{-1}((-\infty, t])$. Since h is self-indexing, $M_{1/2} = S^3$ is the boundary of the unique 0-handle (which is attached at time $t = 0$), $M_{3/2}$ is the boundary of the union of the 0- and 1-handles (attached at time $t = 1$), and $M_{5/2}$ is the boundary of the 0-, 1-, and 2-handles (attached at time $t = 2$).

It can be seen that each 1-handle that is attached changes M_t by a 0-framed Dehn surgery along the corresponding dotted 1-handle circle in \mathcal{K} . Likewise, each 2-handle attachment changes M_t by a Dehn surgery along the corresponding framed 2-handle attaching circle in \mathcal{K} . Thus we can identify $M_{3/2}$ with the result of performing 0-surgery to $S^3 = M_{1/2}$ along the 1-handle attaching circles of \mathcal{K} , and we can identify $M_{5/2}$ with the result of performing Dehn surgery to $M_{3/2}$ along the 2-handle attaching circles of \mathcal{K} .

Now, let (L, B) be a pair consisting of a link L and a finite collection of bands B attached to L , and suppose that (L, B) lies in the complement of a tubular neighborhood of \mathcal{K} , i.e. $(L, B) \subseteq S^3 \setminus \nu(\mathcal{K})$. Then, since (L, B) avoids the 1-handle and 2-handle surgeries, we may think of (L, B) as living simultaneously in $M_{1/2}$, $M_{3/2}$, and $M_{5/2}$.

Definition 6 A *banded unlink diagram* in the Kirby diagram \mathcal{K} is a triple (\mathcal{K}, L, B) , such that

1. (L, B) is a banded link in the complement $S^3 \setminus \nu(\mathcal{K})$ of \mathcal{K} ,
2. L bounds disjointly embedded disks D_- in $M_{1/2}$ that are disjoint from the dotted 1-handle circles, and
3. L_B bounds disjointly embedded disks D_+ in $M_{5/2}$.

We would like to see how we can interpret a banded unlink diagram (\mathcal{K}, L, B) as defining a closed surface Σ embedded in X . To do this, we will define $\Sigma \cap M_{3/2}$ to be union of the link L and the bands B . We would like to extend the surface Σ from this cross-section downwards over $h^{-1}([1/2, 3/2])$ as a product $L \times [1/2, 3/2]$, and upwards over $h^{-1}([3/2, 5/2])$ as a product $L_B \times [3/2, 5/2]$ of the surgered link L_B .

Here, to define the product surfaces $L \times [1/2, 3/2]$ and $L_B \times [3/2, 5/2]$ we are implicitly using product structures on the ambient space which are induced by the Morse function h and its gradient flow. Note that because there are critical points in $h^{-1}([1/2, 3/2])$ and $h^{-1}([3/2, 5/2])$ corresponding to 1-handles and 2-handles of X respectively, the gradient ∇h doesn't induce global product structures on either of these sets. However, if we avoid a neighborhood of the ascending and descending manifolds of these critical points (see Section 3.3 for more details) we obtain product structures $(S^3 \setminus \nu(\mathcal{K})) \times [1/2, 3/2]$ and $(S^3 \setminus \nu(\mathcal{K})) \times [3/2, 5/2]$ on proper subsets of $h^{-1}([1/2, 3/2])$ and $h^{-1}([3/2, 5/2])$ respectively. Since $(L, B) \subseteq S^3 \setminus \nu(\mathcal{K})$, we can use these product structures to define

$$L \times [1/2, 3/2] \subseteq (S^3 \setminus \nu(\mathcal{K})) \times [1/2, 3/2] \subseteq h^{-1}([1/2, 3/2])$$

and

$$L_B \times [3/2, 5/2] \subseteq (S^3 \setminus \nu(\mathcal{K})) \times [3/2, 5/2] \subseteq h^{-1}([3/2, 5/2]).$$

We can therefore extend Σ over these sets by setting

$$\Sigma \cap h^{-1}([1/2, 3/2]) = L \times [1/2, 3/2]$$

and

$$\Sigma \cap h^{-1}([3/2, 5/2]) = L_B \times [3/2, 5/2].$$

We can cap off the surface Σ that we've built so far by adding disks along each remaining boundary component. Since L bounds a family of disks in $M_{1/2} = \partial h^{-1}((-\infty, 1/2])$, we may embed a family of boundary parallel disks D_- in $h^{-1}((-\infty, 1/2])$ whose boundary is $L \subseteq M_{1/2}$. Likewise, since L_B bounds a family of embedded disks in $M_{5/2} = \partial h^{-1}([5/2, \infty))$, we may embed a family of boundary parallel disks D_+ in $h^{-1}([5/2, \infty))$ with boundary $L_B \subseteq M_{5/2}$. Note that the boundary parallel disks (with fixed boundary) in $h^{-1}([5/2, \infty)) = \{3\text{-handles}\} \cup \{4\text{-handles}\}$ are unique up to isotopy rel boundary, just as they are in $h^{-1}((-\infty, 3/2]) \cong B^4$. Thus, we can use the disks D_- and D_+ to cap off our surface on the bottom and top uniquely, giving a closed surface Σ in X .

In summary, the surface Σ is build as follows

$$\begin{aligned} \Sigma \cap h^{-1}([5/2, \infty)) &= D_+ \\ \Sigma \cap h^{-1}((3/2, 5/2]) &= L_B \times (3/2, 5/2] \\ \Sigma \cap h^{-1}(3/2) &= L \cup B \\ \Sigma \cap h^{-1}([1/2, 3/2)) &= L \times [1/2, 3/2) \\ \Sigma \cap h^{-1}((-\infty, 1/2]) &= D_- \end{aligned}$$

See Figure 35 for a schematic of the surface Σ described above.

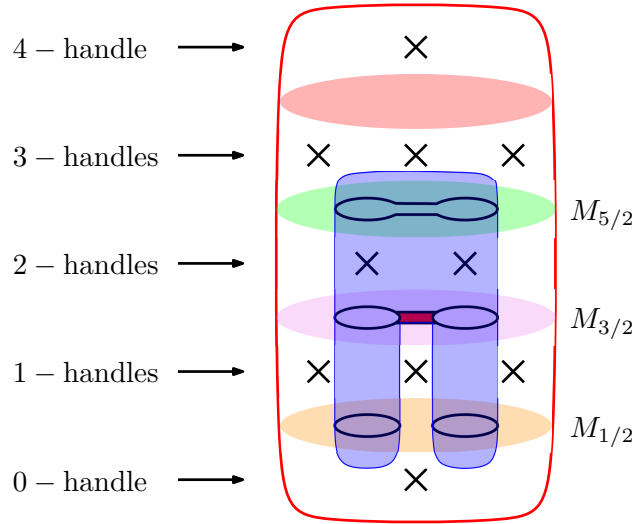


Fig. 35 A schematic of the surface $\Sigma = \Sigma(\mathcal{K}, L, B)$ constructed from the banded unlink diagram (\mathcal{K}, L, B) , where \mathcal{K} is a Kirby diagram for the 4-manifold X .

Given a banded unlink diagram (\mathcal{K}, L, B) , where \mathcal{K} is a Kirby diagram for X , we denote the surface Σ constructed above by $\Sigma(\mathcal{K}, L, B) \subseteq X$. Note that the surface $\Sigma(\mathcal{K}, L, B)$ is uniquely defined up to isotopy by the banded unlink diagram (\mathcal{K}, L, B) , once we've fixed an identification of X with the handle decomposition defined by \mathcal{K} . See Figure 36 for an example of a banded unlink diagram describing a surface in $\mathbb{C}P^2 \# (S^1 \times S^3)$.

3.3 Isotopies of banded unlink diagrams

Now that we have a method for describing knotted surfaces in a 4-manifold equipped with a Morse function or handle decomposition, we'd like to understand to what

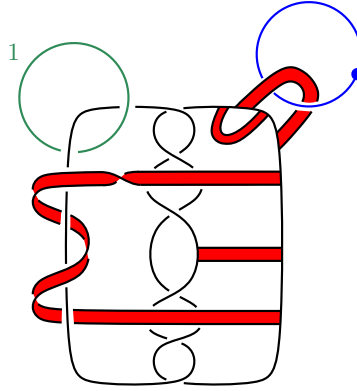


Fig. 36 A banded unlink diagram representing a closed surface in $\mathbb{C}P^2 \# (S^1 \times S^3)$. Note that the unlink L in black bounds a pair of disks in S^3 , while the band-surgered link L_B bounds a pair of disks in $S^1 \times S^2$ (the 3-manifold boundary obtained by performing surgery along the 1- and 2-handle attaching circles).

extent the resulting banded unlink diagrams are uniquely defined. Similar to the situation we encountered with banded unlink diagrams in S^4 , banded unlink diagrams of isotopic surfaces in X may differ by a combination of band slides and band swims. In the general case, however, we also must consider how the surfaces interact with the topology (as captured by the Kirby diagram) of the ambient manifold X . As a result, we also obtain moves which involve sliding or swimming the banded unlink over or through some combination of 1-handle or 2-handle attaching circles, as illustrated in Figure 37. Similar to Swenton's theorem (Theorem 3) for knotted surfaces in S^4 , Theorem 4 established that the moves in Figure 37 (together with isotopy in S^3) are sufficient to relate the banded unlink diagrams of any two isotopic surfaces in X .

Theorem 4 (Hughes-Kim-Miller [9]) *If Σ and Σ' are closed surfaces smoothly embedded in X which are described by banded unlink diagrams (\mathcal{K}, L, B) and (\mathcal{K}, L', B') respectively, then Σ and Σ' are isotopic if and only if (\mathcal{K}, L, B) and (\mathcal{K}, L', B') can be related by a sequence of ambient isotopies and the moves shown in Figure 37.*

A few comments regarding the moves in Figure 37 are in order. Notice that in the moves involving the Kirby diagram the 1- and 2-handles aren't interchangeable. This is because we think of the banded unlink diagram as existing in the $M_{3/2}$ level set, with the 1-handles being added below, and 2-handles being added above. Thus, for example, it's possible to swim a 2-handle attaching circle through a band (right, second row, Figure 37) since the 2-handle is attached after the band surgeries are performed, and hence the 2-handle attaching circle can be isotoped through the lane created by band surgery. The same can't be achieved with a 1-handle dotted circle, as the 1-handle attachments take place before the band surgeries are performed (and thus, there is no gap in the link for the dotted circle to travel through). In fact,

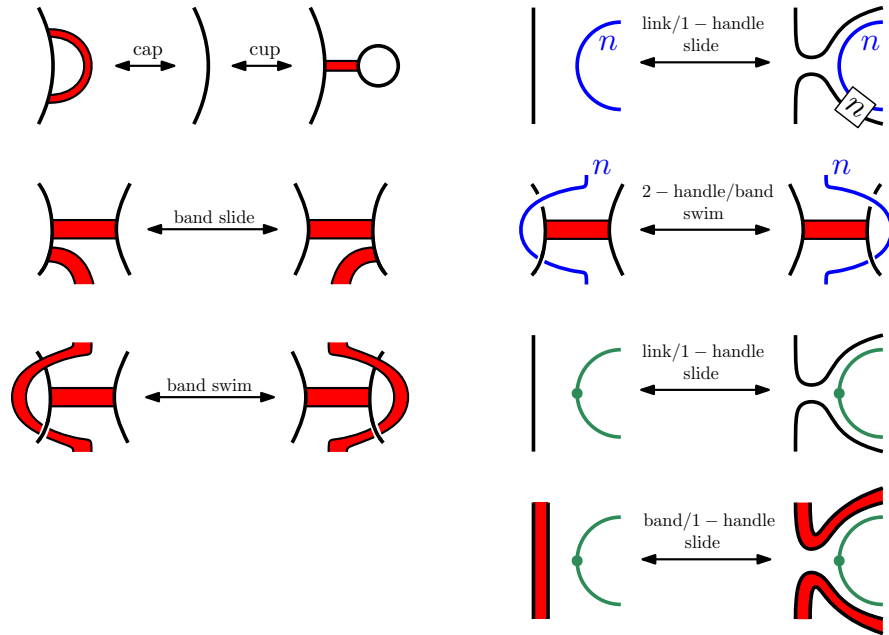


Fig. 37 A full set of moves which, together with isotopy in S^3 , are sufficient to related the banded unlink diagrams of any two isotopic surfaces in X .

swimming a dotted 1-handle circle through a band would involve forcing the link L to travel over the corresponding 1-handle, which cannot be achieved through isotopy of the surface. These points will become more evident as we sketch the proof of Theorem 4 in Section 3.4.

3.4 Sketch of the proof of Theorem 4

Before sketching the proof of Theorem 4 we make a few comments about the proof of Theorem 3, which says that isotopies of knotted surfaces in S^4 can be captured by band moves and isotopies of banded unlink diagrams in S^3 . Recall that given a knotted surface we obtain a banded unlink diagram by pushing all maximum disks up to $t = 1$, pushing all minimum disks down to $t = -1$, and pushing all of the saddle bands to $t = 0$. Given an isotopy of a knotted surface K , we can track the images of the saddle points of K under the projection to time $t = 0$ as the isotopy progresses. Band moves arise at times in the isotopy when the images of two saddle bands intersect under the projection. Furthermore, during the isotopy of K the induced Morse function $\pi|_K : K \rightarrow \mathbb{R}$ may change, and may involve cancellations between pairs of critical points. These critical points pair cancellations give rise to cup moves

(a minimum point cancelling a saddle point) and cap moves (a saddle point cancelling a maximum point).

Proving the same results in an arbitrary closed 4-manifold equipped with a handle decomposition is similar, though more technical. The first step involves making sense of how to project the critical points of a surface K down to a central cross-section. Recall that if $h : X \rightarrow \mathbb{R}$ is a Morse function, and $t_0 < t_1$ are two regular values of h with no critical values in $[t_0, t_1]$, then the gradient flow of $\pm \nabla h$ allows us to identify nearby level sets of h and we obtain a diffeomorphism $h^{-1}([t_0, t_1]) \cong M_{t_0} \times [t_0, t_1]$. In particular, this identification of level allows us to project subsets of M_{t_1} down to M_{t_0} , and vice versa.

Our situation in X is complicated by the fact that we often need to project saddle bands up or down past critical points of h (i.e. handle attachments in X), so we cannot assume that $[t_0, t_1]$ is free of critical values of h . However, if we avoid the critical points in $h^{-1}([t_0, t_1])$, as well as all of the points that would project to those critical points under the flow of $\pm \nabla h$, then we are able to identify the remaining points using $\pm \nabla h$ as before. This fact motivates the following definitions:

Definition 7 Let $h : X \rightarrow \mathbb{R}$ be a Morse function, and let $\varphi_t : X \rightarrow X$ denote the flow of $-\nabla h$. If $p \in X$ is a critical point of h , then we define

- the *ascending manifold* of p is

$$\text{asc}(p) = \{x \in X \mid \lim_{t \rightarrow \infty} \varphi_t(x) = p\}$$

- the *descending manifold* of p is

$$\text{des}(p) = \{x \in X \mid \lim_{t \rightarrow -\infty} \varphi_t(x) = p\}.$$

Note that these are sometimes referred to as the *stable* and *unstable manifolds* of p respectively.

From a handlebody perspective, note that the descending manifold of a critical point corresponds to the core of the associated handle, while its ascending manifold corresponds to its cocore.

Now, back to our surface K embedded in X . By dimensionality arguments we may push K off of the 0-, 3- and 4-handles, and assume that it lives in the union of the 1- and 2-handles of X , which we think of as being attached during the time interval $[1/2, 5/2]$. Because the set $h^{-1}([1/2, 5/2])$ contains critical points the Morse gradient $-\nabla h$ will not induce a global product structure on it. However, if we let W denote the union of the ascending and descending manifolds of the index 1- and 2-critical points of h , then $-\nabla h$ will induce a product structure on $h^{-1}([1/2, 5/2]) \setminus W$, which we denote by $h^{-1}([1/2, 5/2]) \setminus W \cong M_{1/2} \times [1/2, 5/2]$. Thus, for any $t_0, t_1 \in [1/2, 3/2]$ we may identify subsets of $h^{-1}(t_0)$ with subsets of $h^{-1}(t_1)$ as long as they avoid the ascending and descending manifolds of the 1- and 2-handles of X . We can use this identification as a projection function to push the minimum disks of K down to $M_{1/2}$, the maximum disks of K up to $M_{5/2}$, and the

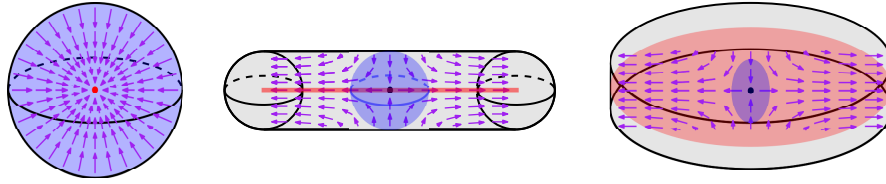


Fig. 38 Ascending manifolds (blue) and descending manifolds (red) of low-index critical points in a 4-manifold. *Left*: An index 0 critical point p , whose descending manifold is just $\{p\}$, and whose ascending manifold is 4-dimensional. *Center*: An index 1 critical point, with 1-dimensional descending manifold and 3-dimensional ascending manifold. *Right*: An index 2 critical point, whose descending and ascending manifolds are both 2-dimensional.

saddle bands of K to $M_{3/2}$. These projections can again be tracked during an isotopy of K to give a set of moves relating the banded unlink diagrams of isotopic surfaces.

Similar to the situation in S^4 , we run into issues when the projection of two bands intersect in $M_{3/2}$. Once again, these intersections give rise to band slides and band swims, as in S^4 . We also obtain cap and cup moves which correspond to the cancelling pairs of critical points of the induced Morse function $h|_K : K \rightarrow \mathbb{R}$.

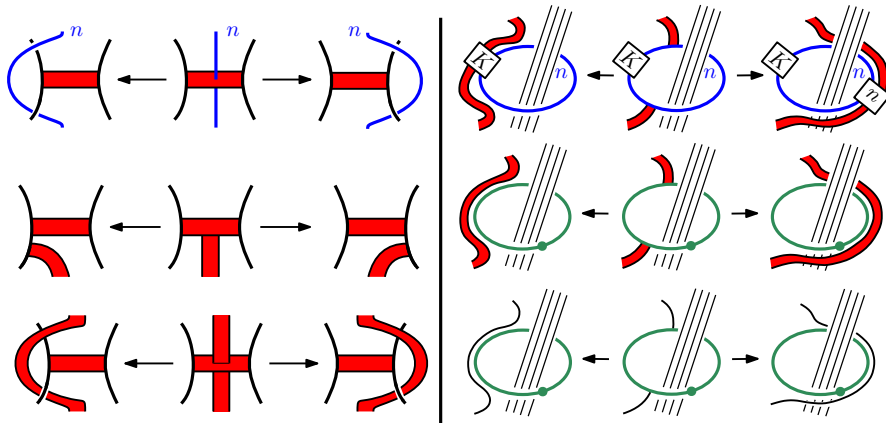


Fig. 39 Situations where the projection of a saddle band or link component may intersect other saddle bands or the ascending/descending manifolds of index 1 and 2 critical points. Each such intersection gives rise to a move between bands, link components, and handles. For the situations on the right, the strands passing through the handle attaching circles represent any combination of link components, handle attaching circles, and bands.

Unfortunately, during an isotopy of K we can't completely avoid the ascending and descending manifolds of all of the index 1 and 2 critical points, and each time a saddle band passes through these manifolds the resulting banded unlink diagram changes by a band/handle move. For example, if a saddle band passes through the

ascending manifold of an index 2-critical point (i.e. the cocore of the corresponding 2-handle) then after pushing that band down to $M_{3/2}$ the resulting banded unlink diagram will differ by a band slide over the 2-handle attaching circle (see top right, Figure 39). Alternatively, if a saddle band passes through the descending manifold of an index 2 critical point during the isotopy (i.e. the core of the corresponding 2-handle), then after pushing that band up to $M_{1/2}$ the resulting banded unlink diagrams will differ by a swim of the attaching circle of the 2-handle through the band (see top left, Figure 39). The two dotted circle moves in Figure 37 correspond to sliding part of the surface, either a link component or band, underneath a 1-handle (i.e. in between the two 3-balls which make up the attaching region of the handle). See the center and bottom right illustrations in Figure 39.

3.5 Banded unlink diagrams for immersed surfaces

In this final section we briefly discuss how banded unlink diagrams can be modified to described immersed surfaces in 4-manifolds. The main difference from the surfaces we've considered previously is that immersed surfaces may have self-intersections which must be represented in our diagrams.

Suppose then that K is a surface which is immersed in X . After a small perturbation of K we may assume that it is embedded away from a finite set of transverse double points. Similar to how we pushed all of the saddle bands of our surfaces to the central cross-section $M_{3/2} = h^{-1}(3/2)$ in the embedded setting, through ambient isotopy of X we can also arrange for the self-intersections of K to all sit inside $M_{3/2}$. This results in a singular banded link (L, B) , in which the link L may have transverse double points. Away from the $M_{3/2}$ level the surface K is embedded.

In the language of motion pictures, a transverse double point of K will be observed as a crossing change in the link diagrams of the level sets. As t increases, one strand of the surface will approach another, before the two strands pass through each other precisely at time $t = 3/2$, before they separate again (see Figure 40).

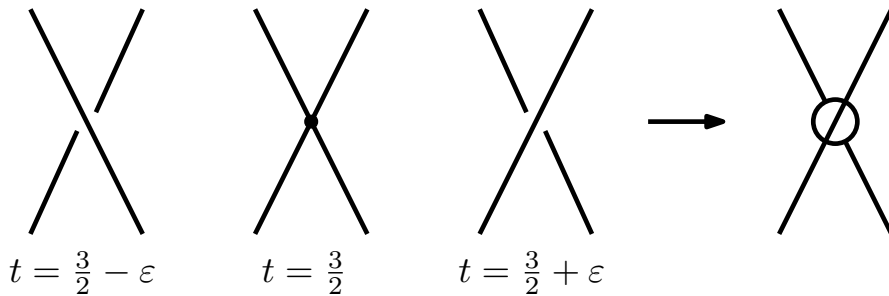


Fig. 40 A motion picture in a neighborhood of a singular point. The local intersection information is recorded by decorating the singular point in the banded unlink diagram as above.

We will record this local crossing information at each self-intersection of K by adding a decorated vertex at each singular point of the banded link (L, B) . By choosing the direction of the vertex appropriately as in Figure 40, we can record which strand is pushed above the other when we move slightly forward in time from the singular banded unlink at time $t = 3/2$. In other words, we orient each decorated vertex so that the motion picture of K looks locally like Figure 40 in a neighborhood of each self-intersection, when read from left to right. Let L^- denote the link we obtain from L by resolving each vertex as in the left of Figure 40, and let L^+ denote the link we obtain from L by resolving each vertex as in the right of Figure 40.

We can now define the notion of a singular banded unlink diagram similar to a banded unlink diagram. The only difference is that now, in addition to performing the band surgeries at time $t = 3/2$, we must also perform crossing changes as prescribed by the vertex decorations:

Definition 8 A *singular banded unlink diagram* in the Kirby diagram \mathcal{K} is a triple (\mathcal{K}, L, B) such that

1. (L, B) is a singular banded link in the complement $S^3 \setminus \nu(\mathcal{K})$ of \mathcal{K} , where each singular point of L is decorated with a vertex as in Figure 40,
2. L^- bounds disjointly embedded disks in $M_{1/2}$ which are disjoint from the dotted 1-handle circles, and
3. L_B^+ bounds disjointly embedded disks in $M_{5/2}$.

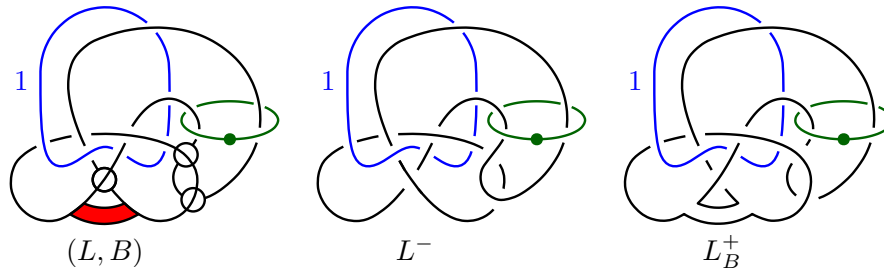


Fig. 41 *Left:* A singular banded unlink diagram of a singular sphere in $\mathbb{C}\mathbb{P}^2 \# (S^1 \times S^3)$. *Center and right:* We draw the resolved links L^- and L_B^+ , which can be thought of as the cross-sections of the surface at heights $t = 3/2 - \varepsilon$ and $t = 3/2 + \varepsilon$ respectively.

Given a singular banded unlink diagram we can construct an immersed surface very similar to how we constructed embedded surfaces before. After resolving the singular crossings and band surgeries locally in a neighborhood of $M_{3/2}$, we extend the resulting surfaces as a product to $M_{1/2}$ and $M_{5/2}$, before capping off with boundary parallel disks in $h^{-1}((-\infty, 1/2])$ and $h^{-1}([5/2, -\infty))$.

As before, we also obtain a set of moves which are sufficient to relate any two singular banded unlink diagrams of isotopic surfaces. In addition to the ordinary band/handle swims and slides which we saw in Theorem 4, we also obtain moves

which involve the decorated singular vertices and the bands. We summarize this result in our final theorem:

Theorem 5 (Hughes-Kim-Miller [8]) *If Σ and Σ' are closed surfaces smoothly immersed in X which are described by singular banded unlink diagrams (\mathcal{K}, L, B) and (\mathcal{K}', L', B') respectively, then Σ and Σ' are ambiently isotopic if and only if (\mathcal{K}, L, B) and (\mathcal{K}', L', B') can be related by a sequence of ambient isotopies and the moves shown in Figures 37 and 42.*

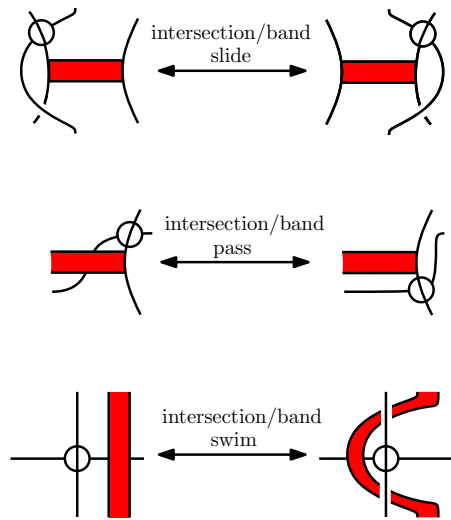
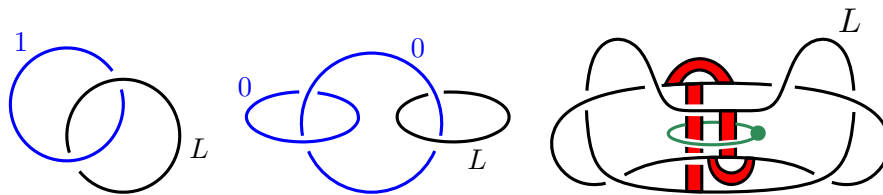


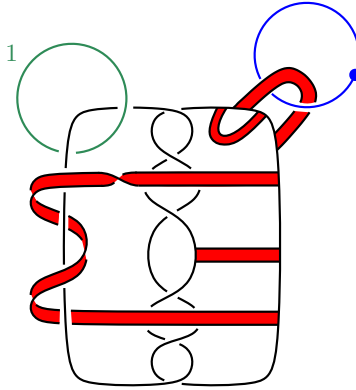
Fig. 42 Together with the moves in Figure 37, the above moves are sufficient to relate the singular banded unlink diagrams of any two ambiently isotopic immersed surfaces.

Exercises

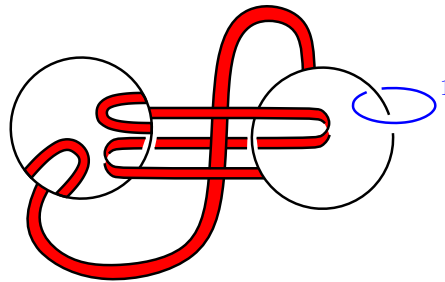
3.1. Can you identify the following 4-manifolds and embedded surfaces?



- 3.2. Verify that the following diagram is a banded unlink diagram (i.e. check that the link L in black bounds a family of embedded disks in $M_{1/2}$, and that the surgered link L_B bounds a family of embedded disks in $M_{5/2}$). What is the topological type of the resulting surface? Can you describe the resulting surface as a connected sum of simpler surfaces in S^4 , $\mathbb{C}P^2$, and $S^1 \times S^3$?



- 3.3. Show that the surface below is the connected sum of an unknotted torus T in S^4 with $\mathbb{C}P^1$ inside $\mathbb{C}P^2$.



- 3.4. In this exercise you will prove a fact that is needed to show that banded unlink diagrams in X^4 can be capped off uniquely.

Consider $\natural_k(S^1 \times B^3)$, i.e. the boundary sum of k copies of $S^1 \times B^3$. We can think of $\natural_k(S^1 \times B^3)$ as being the 3- and 4-handles of a handle decomposition of X , and $\partial(\natural_k(S^1 \times B^3)) = \sharp_k(S^1 \times S^2)$ as being the level set $M_{5/2}$ of X .

Suppose that E and E' are two sets of boundary parallel disks properly embedded in $\natural_k(S^1 \times B^3)$ with the same boundary. Show that E and E' are isotopic rel boundary. (Hint: Can you isotope both E and E' so that they live inside some 4-ball inside of $\natural_k(S^1 \times B^3)$?)

- 3.5. Show that the diagram on the left of Figure 41 is a valid singular banded unlink diagram, and that it defines a sphere immersed in $\mathbb{C}P^2 \# (S^1 \times S^3)$.

Acknowledgements These notes are based on a minicourse that the author gave at the 2024 Georgia Topology Conference. The author would like to thank the organizers of this conference for their hospitality and for organizing such a stimulating conference. Some of the topics and exercises in these notes were based on material for a course Maggie Miller taught on knotted surfaces at the University of Texas at Austin, and the author is indebted to her for sharing these materials. The author also thanks Geunyoung Kim and Seungwon Kim for helpful comments and discussions during the development of the minicourse. The author was supported by the NSF (DMS-2213295).

References

1. Selman Akbulut. *4-manifolds*, volume 25. Oxford University Press, 2016.
2. Kawauchi Akio, Shibuya Tetsuo, and Suzuki Shin'ichi. Descriptions on surfaces in four-space in normal forms. In *Mathematics seminar notes*, volume 10, pages 75–125, 1982.
3. Emil Artin. Zur isotopie zweidimensionaler flächen im \mathbb{R}^4 . In *Abhandlungen aus dem Mathematischen Seminar der Universität Hamburg*, volume 4, pages 174–177. Springer, 1925.
4. J Scott Carter and Masahico Saito. *Knotted surfaces and their diagrams*, volume 55. American Mathematical Society, 2023.
5. Scott Carter, Seiichi Kamada, and Masahico Saito. *Surfaces in 4-space*, volume 142. Springer Science & Business Media, 2013.
6. RH Fox. Rolling. 1966.
7. Robert E Gompf and András I Stipsicz. *4-manifolds and Kirby calculus*, volume 20. American Mathematical Society, 2023.
8. Mark Hughes, Seungwon Kim, and Maggie Miller. Band diagrams of immersed surfaces in 4-manifolds. *arXiv preprint arXiv:2108.12794*, 2021.
9. Mark C Hughes, Seungwon Kim, and Maggie Miller. Isotopies of surfaces in 4-manifolds via banded unlink diagrams. *Geometry & Topology*, 24(3):1519–1569, 2020.
10. Seiichi Kamada. *Braid and knot theory in dimension four*, volume 95. American Mathematical Soc., 2002.
11. Seiichi Kamada. *Surface-knots in 4-space*. Springer, 2017.
12. Cherry Kearton and Vitaliy Kurlin. All 2-dimensional links in 4-space live inside a universal 3-dimensional polyhedron. *Algebraic & Geometric Topology*, 8(3):1223–1247, 2008.
13. Richard A Litherland. Deforming twist-spun knots. *Transactions of the American Mathematical Society*, 250:311–331, 1979.
14. Inasa Nakamura. Showing distinctness of surface links by taking 2-dimensional braids. *Pacific Journal of Mathematics*, 278(1):235–251, 2015.
15. Patrick Naylor and Hannah R Schwartz. Gluck twisting roll spun knots. *Algebraic & Geometric Topology*, 22(2):973–990, 2022.
16. Dennis Roseman. Reidemeister-type moves for surfaces in four-dimensional space. *Banach Center Publications*, 42(1):347–380, 1998.
17. Frank J Swenton. On a calculus for 2-knots and surfaces in 4-space. *Journal of Knot Theory and Its Ramifications*, 10(08):1133–1141, 2001.
18. Katsuyuki Yoshikawa. An enumeration of surfaces in four-space. 1994.
19. E Christopher Zeeman. Twisting spun knots. *Transactions of the American Mathematical Society*, 115:471–495, 1965.